THE ASTROPHYSICAL JOURNAL, 323:243-262, 1987 December 1

QUASAR ENERGY DISTRIBUTIONS. I. SOFT X-RAY SPECTRA OF QUASARS

BELINDA J. WILKES AND MARTIN ELVIS
Harvard-Smithsonian Center for Astrophysics
Received 1986 October 8; accepted 1987 May 22

ABSTRACT

As the initial stage of a study of quasar energy distributions (QEDs) we present *Einstein* IPC spectra of 24 quasars. We combine these with previously reported IPC spectra to form a sample of 33 quasars with well-determined soft X-ray slopes. The best-fit power-law slopes ($f_\nu \propto \nu^{-\alpha_E}$) have a wide range ($-0.2 \leq \alpha_E \leq 1.8$) but are strongly grouped around values of ~ 0.5 for radio-loud quasars and ~ 1.0 for radio-quiet quasars. A correlation analysis shows that radio loudness ($f_{\rm radio}/f_B$), rather than redshift or luminosity, is fundamentally related to the X-ray slope. This correlation is not followed by higher energy spectra of active galaxies. Two components are required to explain both sets of results. The best-fit column densities are systematically smaller than the Galactic values. The same effect is not present in a sample of BL Lac objects, implying that the effect is intrinsic to the quasars and is caused by a low-energy turnup in the quasar spectra.

Subject headings: BL Lacertae objects — quasars — spectrophotometry — X-rays: spectra

I. INTRODUCTION

The highly luminous "nonthermal" continuum of quasars extends from the far-infrared to the hard X-ray (and perhaps γ-ray) energies, emitting roughly constant luminosity per decade of frequency (Carleton *et al.* 1987; Bezler *et al.* 1984). Our understanding of the physical mechanisms producing this continuum is still primitive. In part this is due to the need to use many different instruments to cover the full range of this broad continuum. We have initiated a program to study quasar energy distributions (QEDs) over the full range of the observable spectrum for a unique sample of quasars with good X-ray data. Information on the X-ray region, in particular, has been limited for the most part to single broad-band luminosities integrated over logarithmic bandwidths comparable to the entire combined optical and ultraviolet regions. The role of X-rays as part of the overall energy distribution can only be understood when this information is expanded to include a knowledge of the spectral shape in the X-ray band. This paper helps to fill this need by presenting a survey of X-ray spectra of quasars from the *Einstein* satellite (Giacconi *et al.* 1979).

The first *Einstein* imaging proportional counter (IPC) (Gorenstein, Harnden, and Fabricant 1981) spectra of quasars (Elvis, Wilkes, and Tananbaum 1985; Elvis *et al.* 1986) showed a wide range of slopes for the continuum in the soft X-ray region (0.2–3.5 keV). This contrasts markedly with earlier spectral data. Observations of about 30 active galaxies (AGNs), mainly Seyfert 1's at harder energies (2–20 keV), showed a tight uniformity in their spectral index ($f_\nu \propto \nu^{-\alpha_E}$) $\alpha_E = 0.65 \pm 0.15$ (Mushotzky 1984). The small number of objects in these first IPC samples, while sufficient to demonstrate that the quasars looked different at soft energies, precluded any statistical investigation. It is unclear, for example, whether a continuous range of X-ray slopes exists or whether quasars divide into discrete subsamples. The soft X-ray slope may also depend upon other properties of the quasar such as optical or radio flux or redshift. In an attempt to answer these and other open questions, we have made a survey of IPC spectra including all quasars in the *Einstein* data bank that are not optically violent variables. We report here all those with sufficient signal-to-noise ratio (S/N) to yield a well-constrained spectral slope: a sample of 24 quasars. Combined with those quasars presented in the earlier papers (Elvis, Wilkes, and Tananbaum 1985; Elvis *et al.* 1986), this yields a sample of 33 objects with which to study the X-ray emission of quasars and the relationship of the X-ray spectrum to their other properties.

Throughout the paper a Friedmann cosmology with $q_0 = 0$ and $H_0 = 50$ km s^{-1} Mpc^{-1} is adopted.

II. OBSERVATIONS AND ANALYSIS

a) *The Sample*

As described in Elvis, Wilkes, and Tananbaum (1985), spectral fits may be determined for any object observed on-axis with the IPC, since here the gain of the detector is known to good accuracy. Useful constraints upon the spectral characteristics are obtained only when the statistical errors are sufficiently low; we therefore examined all quasar observations in the *Einstein* data bank in 1985 May having $\gtrsim 300$ total counts (i.e., a signal-to-noise ratio $\gtrsim 10$). Our present sample contains 51 quasars for which spectral fits have been obtained. We have excluded two optically violent variables (OVVs) from this sample (3C 345, 3C 446) since, together with BL Lac objects, they seem to form a physically different set of objects (Angel and Stockman 1980). The number of objects will increase somewhat when the survey is expanded to include all data bank observations and also observations which require specialized processing before spectral fits may be obtained (e.g., the inclusion of high-background data). Although there is no direct selection effect, the sample is necessarily biased toward quasars with little intrinsic absorbing column, since sufficient observed counts over the full energy response of the IPC are necessary to obtain a spectral fit (Elvis, Wilkes, and Tananbaum 1985). It is also biased against relatively X-ray–quiet (i.e., steep α_{ox}) quasars. This is demonstrated in Figure 1, where the α_{ox} (effective optical to X-ray slope) distribution of this sample is compared with that of the optically selected Palomer-Green (PG) sample (Tananbaum *et al.* 1986). Values of α_{ox} are taken from Tananbaum *et al.* (1983), Tananbaum *et al.* (1986), and Zamorani *et al.* (1981). They are unavailable for two of the quasars.

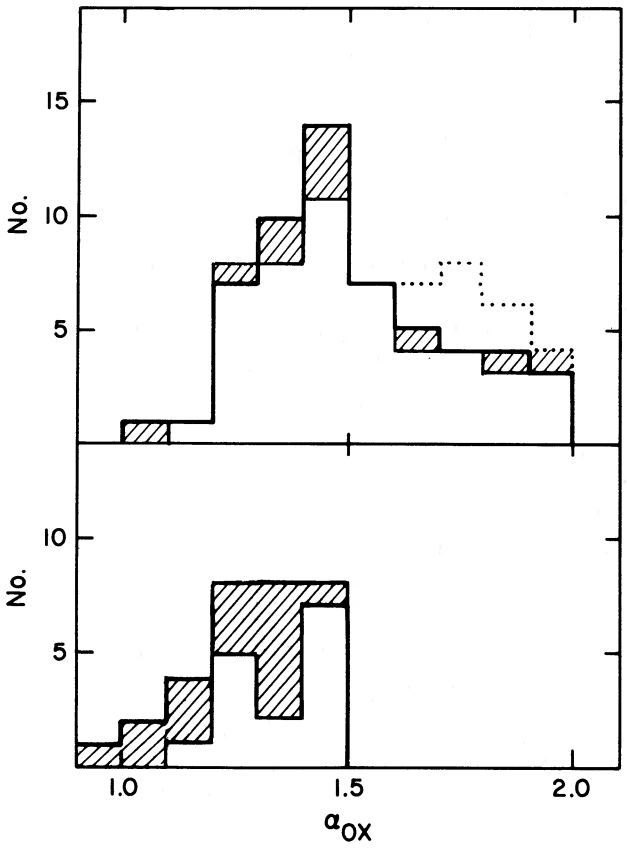

FIG. 1.—Distribution of α_{ox} for PG sample (Tananbaum *et al.* 1986) (*top*) compared with that for current sample (*bottom*). Lower limits are indicated by a dotted line; radio-loud objects are shaded.

In this paper we present new X-ray data for 24 quasars. These are combined with the three objects discussed by Elvis, Wilkes, and Tananbaum (1985) and six from Elvis *et al.* (1986) to yield a sample of 33 quasars which is presented in Table 1. The majority of these observations gave well-determined, soft X-ray spectral indices (total error, 90% confidence, <1.3). Details of the X-ray observations are presented in Table 2. Five quasars with poorly constrained slopes have been included in our analysis: 0007+107, 0312−770, 1407+265, 1416−129, and 1635+119. These objects are potentially important for extending the dynamic range in X-ray luminosity of our sample since they are either X-ray luminous ($L_x > 10^{45}$ ergs^{-1}) and radio quiet or X-ray faint and radio loud (see § III*d*). In six cases several IPC observations were combined to improve the spectral fit over that for a single observation (see next section); each observation is listed individually in Table 2. It is notable that count rates presented here may differ from those reported in earlier papers due to the use of different X-ray data and the different energy range over which counts were accumulated.

For the remaining 18 quasars, the 90% confidence limits give a total error in spectral index of >1.3 and thus are not useful in constraining the X-ray slope. The dominant cause of the poor constraints is lower signal-to-noise observations. However, other factors which may contribute include a high Galactic absorbing column [of six quasars with N_H(Gal) $> 5.0 \times 10^{20}$ cm^{-2}, only one gave a well constrained fit, $\Delta\alpha = 1.3$] and a high intrinsic absorbing column (total $N_H \gtrsim 1 \times 10^{21}$ cm^{-2}), also, while the high S/N requirement favors steep slopes, if the spectral index is too steep there are insufficient counts in the high-energy IPC channels. It is clear that, although no well-defined selection effects are present, a variety of different factors conspire to limit the range of objects we include. We do not expect our sample to be representative of quasars as a class and it is likely that it does not include a full range of spectral indices. The extent of our coverage of α_E and N_H space is being investigated further.

b) IPC Spectral Fitting

The X-ray spectra were analyzed as described in Elvis *et al.* (1986). Briefly, source counts were extracted using a 3′ circle centered on the source position and corrected for counts falling outside this circle based upon the point response function as a function of pulse height. Background counts, which are almost always negligible, were estimated from a 5′–6′ annulus also centered upon the source position. Counts were extracted in each case for those channels most closely approximating the observed energy range 0.1–3.5 keV. The lowest energy pulse-height channel was excluded from the fit in cases where the errors were high.

There are a number of model emission spectra which could reasonably be applied to the soft X-ray data of quasars including power-law, thermal-bremsstrahlung, thermal-plasma (Raymond and Smith 1977), and blackbody spectra. The limited energy resolution of the IPC makes it difficult to distinguish between these alternatives, although the latter two models tend to produce the poorest fits (Elvis *et al.* 1986). For this reason, and following the practice in Elvis *et al.* (1986), we will discuss our results solely in terms of the simplest model, that of a power law. Both the power-law index and the equivalent hydrogen column density of absorbing cold matter were allowed to vary without restriction yielding two-dimensional confidence contours from which limits could be placed on both parameters.

Several of the quasars were observed more than once by the IPC. All observations with sufficient signal-to-noise ratio were analyzed individually as described above. In these cases the observation yielding the strongest constraint on spectral parameters is reported here. In addition, for six objects repeated observations were separated by a few days (less than two weeks in all cases) and no significant evidence for spectral variability during this period was found. These multiple fields were combined to improve constraints on the spectral characteristics of the data. Two of these quasars, 1416−129 and 1426+015, were discussed in Elvis *et al.* (1986) from a single observation. Since the current analysis includes new data, the new spectral fits are reported in full in this paper. The two observations for 1635+119 give comparable count rates and were summed despite a time lag of 1 yr (Table 2). This improved an otherwise extremely poor fit for this important object.

It should be noted that Zamorani *et al.* (1984) report significant variability between the two observations of 1635+119, which is not apparent in our data. Zamorani *et al.* (1984) also reported intermediate time scale flux variability for three objects in our sample: Mrk 205, 3C 273, PG 1416−129. While we do not find strong evidence for spectral variability on this same time scale, we note that our results necessarily represent a mean over the period covered by these data. A detailed study of variability will be presented in a later paper.

An additional source of error in the spectral fitting procedure is the uncertainty in the gain of the IPC, estimated as

TABLE 1

THE QUASAR SAMPLE

Object	N_H(21 cm)[a]	z	Apparent B Magnitude[b]	$4\pi d^2$ (10^{56} cm^2)	α_{ox}
0007+107 (PG, III Zw 2)	5.8	0.089	15.96 (SG)	0.37	1.14
0026+129 (PG)	4.6	0.142	15.70 SG)	1.00	1.29
0054+145 (PHL 909)	4.9	0.171	16.60 (HB)	1.48	1.28
0133+207 (3C 47)	5.7	0.425	18.15 (HB)	11.42	0.98
0134+329 (3C 48)	4.5	0.367	16.25 (HB)	8.11	1.35
0205+024 (NAB)	3.4	0.155	15.74 (HB)	1.20	1.46
0312−770 (PKS)	3.0	0.223	16.26 (HB)	2.64	1.30
0637−752 (PKS)	5.0	0.656	16.08 (HB)	32.64	1.24
0903+169 (3C 215)	3.6	0.411	18.48 (HB)	10.56	1.13
0923+392 (4C 39.25)	1.5	0.699	17.92 (HB)	38.27	1.12
1028+313 (B2)	2.0	0.177	17.07 (HB)	1.60	1.14
1100+773 (3C 249.1)	3.9	0.311	15.70 (HB)	5.55	1.40
1116+215 (PG)	1.3	0.177	15.17 (SG)	1.60	1.49
1137+661 (3C 263)	1.0	0.656	16.50 (HB)	32.64	1.34
1146−037 (PKS)	2.5	0.341	16.96 (HB)	6.85	1.19
1202+281 (PG, GQ Comae)	1.7	0.165	15.70 (HB)	1.37	1.33
1211+143 (PG)	2.7	0.085	14.63 (SG)	0.34	1.39
1217+023 (PKS)	1.9	0.24	16.55 (HB)	3.11	1.16
1219+756 (Mrk 205)	3.4	0.07	15.64 (VV)	0.23	1.21
1226+023 (3C 273)	1.8	0.158	13.07 (HB)	1.25	1.30
1253−055 (3C 279)	2.1	0.538	18.01 (HB)	20.05	1.03
1307+085 (PG)	2.1	0.158	15.28 (HB)	1.25	1.43
1407+265 (PG)	1.5	0.944	15.73 (SG)	83.06	1.44
1416−129 (PG)	6.8	0.129	15.40 (SG)	0.81	1.26
1426+015 (PG)	2.8	0.086	15.05 (SG)	0.35	1.36
1501+106 (Mrk 841, PG)	2.4	0.036	14.50 (VV)	0.06	1.30
1545+210 (3C 323.1)	4.3	0.266	16.80 (HB)	3.91	1.14
1613+658 (PG)	2.9	0.129	15.66 (HB)	0.81	1.32
1635+119	4.5	0.146	16.98 (HB)	1.06	1.32
1721+343 (4C 34.47)	3.0	0.206	16.52 (HB)[c]	2.22	1.05
1803+676 (Kaz 102)	4.7	0.136	16.04 (HB)	0.91	1.37
2130+099 (PG, II Zw 136)	4.6	0.061	14.92 (HB)	0.17	1.52
2135−148 (PHL 1657)	4.6	0.20	15.63 (HB)	2.08	1.32

[a] The 21 cm Hydrogen column density due to the Galaxy interpolated from Stark *et al.* (1987) in units of 10^{20} atoms cm^{-2}.

[b] The letters in parentheses are references to the following: HB, Hewitt and Burbidge 1987; SG, Schmidt and Green 1983; VV, Véron-Cetty and Véron 1984.

[c] V magnitude only available.

± 0.2 on a value of between 12 and 15 (Harnden *et al.* 1984). We tested the effect of changing the mean gain by multiples of this amount on the spectral fits for an observation. The results changed by a negligible amount, irrespective of the value of the mean gain, in comparison with the errors intrinsic to the data itself. We have therefore neglected the gain uncertainty in the following analysis.

It should be noted that the IPC gain is not well calibrated above a value of ~ 19 since such high values of gain were rarely recorded after the first few months of the mission (Harnden *et al.* 1984). One quasar in our sample, 3C 47, was observed with the instrument in a high-gain state (see Table 2). Consequently, the quoted errors for this quasar may be underestimated. Three observations of 3C 47, all with different gain, give consistent values for the X-ray slope, giving credibility to our result. Only two of these observations are used here, as the third was taken 1.5 yr later.

The two-dimensional χ^2 contour plots for a single power-law model with spectral slope α_E and equivalent hydrogen absorbing column N_H are given in Figure 2 for the 24 new and two refitted objects; the three contours represent 68%, 90%, and 99% two-parameter confidence limits. The absorbing column due to our galaxy, determined from radio measurements (Stark *et al.* 1987), and the 90% error due to small-scale fluctuations and stray radiation (Elvis *et al.* 1986, Appendix B) are also indicated. Spectral parameters derived from the fitting routine, corresponding to summed multiple sequences where relevant, are given in Table 3 for all the quasars in the combined sample. Values are quoted to one decimal place and errors at the 90% confidence level. The number of degrees of freedom depends upon the pulse-height channels used to extract the data (given in Table 2). It should be noted that α_E and N_H are not independent so that only certain combinations of α_E and N_H within the quoted range lie inside the 90% confidence region. This is shown clearly by the contours in Figure 2. Each quasar from the earlier papers was reanalyzed for this study to ensure consistent treatment for the whole sample. Any small differences between the values in Table 3 and those presented earlier (Elvis, Wilkes, and Tananbaum 1985; Elvis *et al.* 1986) lie well within the errors. The distribution of χ^2_{min} for the sample is consistent with that expected by chance ($p \sim 0.1$ using a Kolmogorov-Smirnov [K-S] test). Thus, despite high values of χ^2 for a few objects, there is no indication from the fits that a single power law is not an adequate representation of the quasar spectra. We have not, unlike in the earlier papers, further constrained the spectral parameters by requiring that the column density of neutral hydrogen exceed the minimum value of the Galactic column as determined from radio mea-

TABLE 2

DETAILS OF IPC X-RAY OBSERVATIONS

Object	Sequence Number	Date	NET Counts, Error	Exposure (s)	Count Rate (s^{-1})	Gain	PHA Channels
0007+107	6718	1980 Jan 9	854 ± 31	2476	0.34 ± 0.01	15.53	2–11
0026+129	5417	1981 Jan 4	509 ± 24	2202	0.23 ± 0.01	12.60	
	9550	1981 Jan 4	521 ± 24	2203	0.24 ± 0.01	12.80	
	9551	1981 Jan 4	505 ± 24	2210	0.23 ± 0.01	12.80	
	9552	1981 Jan 4	495 ± 23	1984	0.25 ± 0.01	12.93	
	9553	1981 Jan 4	587 ± 26	2553	0.23 ± 0.01	12.99	
	Σ		2618 ± 54	11152	0.23 ± 0.01		1–9
0054+145	5418	1980 Jul 19	1282 ± 40	11735	0.11 ± 0.00	15.14	2–11
0133+207	482	1979 Jan 12	234 ± 17	1754	0.13 ± 0.01	25.60	
	540	1979 Jan 12	339 ± 20	2428	0.14 ± 0.01	20.48	
	Σ		573 ± 26	4182	0.14 ± 0.01		4–15
0134+329	480	1980 Jul 25	751 ± 30	7036	0.11 ± 0.00	15.00	2–10
0205+024	3978	1979 Jul 20	1410 ± 41	7608	0.19 ± 0.01	13.70	2–10
0312−770	5401	1979 Nov 8	261 ± 20	2120	0.12 ± 0.01	18.40	3–12
0637−752	8494	1980 Dec 14	1199 ± 39	7480	0.16 ± 0.01	14.00	2–10
0903+169	481	1979 Oct 26	636 ± 32	13459	0.05 ± 0.00	18.47	3–12
0923+392	554	1979 Oct 19	1020 ± 37	9819	0.10 ± 0.00	17.20	2–11
1028+313	4256	1979 May 24	1304 ± 40	6595	0.20 ± 0.01	11.80	2–9
1100+773	478	1979 Apr 27	574 ± 27	3638	0.16 ± 0.01	15.92	2–11
1116+215	5339	1979 Dec 6	425 ± 23	1888	0.23 ± 0.01	12.60	1–9
1137+661	5421	1980 Apr 20	1123 ± 38	10427	0.11 ± 0.00	15.72	2–11
1146−037	5411	1981 Jan 6	251 ± 17	1706	0.15 ± 0.01	12.40	1–9
1202+281	4258	1979 Mar 23	959 ± 32	4176	0.23 ± 0.01	11.80	2–9
1211+143	5341	1980 Dec 11	2290 ± 49	1795	1.28 ± 0.03	14.10	2–10
1217+023	532	1979 Jun 20	659 ± 27	2136	0.31 ± 0.01	13.32	2–9
1219+756	5424	1980 Apr 20	6434 ± 85	13113	0.49 ± 0.01	15.69	2–11
1226+023	2037	1979 Jun 20	4534 ± 68	1740	2.60 ± 0.04	13.93	2–10
1253−055	4645	1980 Jul 14	3191 ± 63	25095	0.13 ± 0.00	15.23	2–11
1307+085	5344	1981 Jan 27	598 ± 26	2149	0.28 ± 0.01	17.60	2–12
1407+265	5381	1981 Jan 17	239 ± 17	1557	0.15 ± 0.01	12.17	1–9
1416−129	10387	1981 Jan 31	536 ± 24	1821	0.29 ± 0.01	17.88	
	10389	1981 Feb 2	596 ± 25	2021	0.29 ± 0.01	18.04	
	Σ		1132 ± 35	3842	0.29 ± 0.01		3–12
1426+015	10374	1981 Jan 4	836 ± 31	2258	0.37 ± 0.01	12.80	
	10390	1981 Jan 5	888 ± 31	2571	0.35 ± 0.01	13.00	
	10391	1981 Jan 5	968 ± 32	2713	0.36 ± 0.01	13.20	
	10392	1981 Jan 5	1039 ± 34	2788	0.37 ± 0.01	13.00	
	10393	1981 Jan 5	1196 ± 37	2879	0.42 ± 0.01	12.81	
	Σ		4927 ± 74	13209	0.37 ± 0.01		2–9
1501+106	6713	1980 Jan 18	1663 ± 41	1475	1.13 ± 0.03	16.80	2–11
1545+210	2054	1979 Aug 13	430 ± 23	1912	0.22 ± 0.01	16.40	
	2055	1979 Aug 30	323 ± 19	1541	0.21 ± 0.01	12.60	
	Σ		753 ± 30	3453	0.22 ± 0.01		2–10
1613+658	10375	1981 Feb 6	298 ± 19	998	0.30 ± 0.02	17.20	
	10394	1981 Feb 6	567 ± 25	1721	0.33 ± 0.01	17.40	
	10395	1981 Feb 6	503 ± 25	1748	0.29 ± 0.01	17.40	
	10396	1981 Feb 9	356 ± 20	1284	0.28 ± 0.02	17.94	
	10397	1981 Feb 10	416 ± 22	1459	0.29 ± 0.02	18.37	
	Σ		2140 ± 50	7210	0.30 ± 0.01		2–12
1635+119	567	1979 Mar 6	278 ± 21	3708	0.07 ± 0.01	14.08	
	5425	1980 Mar 8	442 ± 28	7428	0.06 ± 0.00	16.21	
	Σ		730 ± 35	11136	0.07 ± 0.00		2–11
1721+343	3975	1979 Aug 26	777 ± 29	1545	0.50 ± 0.02	19.19	3–13
1803+676	4265	1979 Jun 16	622 ± 29	7125	0.09 ± 0.00	17.34	2–12
2130+099	1972	1981 Apr 20	862 ± 33	4987	0.17 ± 0.01	16.40	2–11
2135−148	5426	1980 May 10	2521 ± 54	12902	0.20 ± 0.00	16.07	2–11

surements. It was found during our analysis that this constraint may be misleading when combined with such a simple model spectrum (see § III*a*).

Both monochromatic and, to a lesser extent, broad-band derived fluxes are sensitive to the assumed spectral slope over the band-width of the IPC. In Table 3 we also present 1 keV monochromatic and 0.3–3.5 keV broad-band fluxes (observed frame), derived and corrected for absorption using the maximum and minimum 90% confidence limits on α_E and N_H. These values generally correspond to 90% confidence limits on the flux. The second row of figures, in parentheses, are the "observed" values; i.e., they are not corrected for absorption. In the final column, the derived, rest frame, broad-band (0.3–3.5 keV) luminosity is given. The errors quoted throughout this table are the result of combining the errors due to the 90% confidence limits upon the spectral parameters with the statistical errors on the total counts of the observation (Table 2).

III. DISCUSSION

Combining the sample presented here with the three sources discussed in Elvis, Wilkes, and Tananbaum (1985) and the six in Elvis *et al.* (1986), which have well-determined spectral

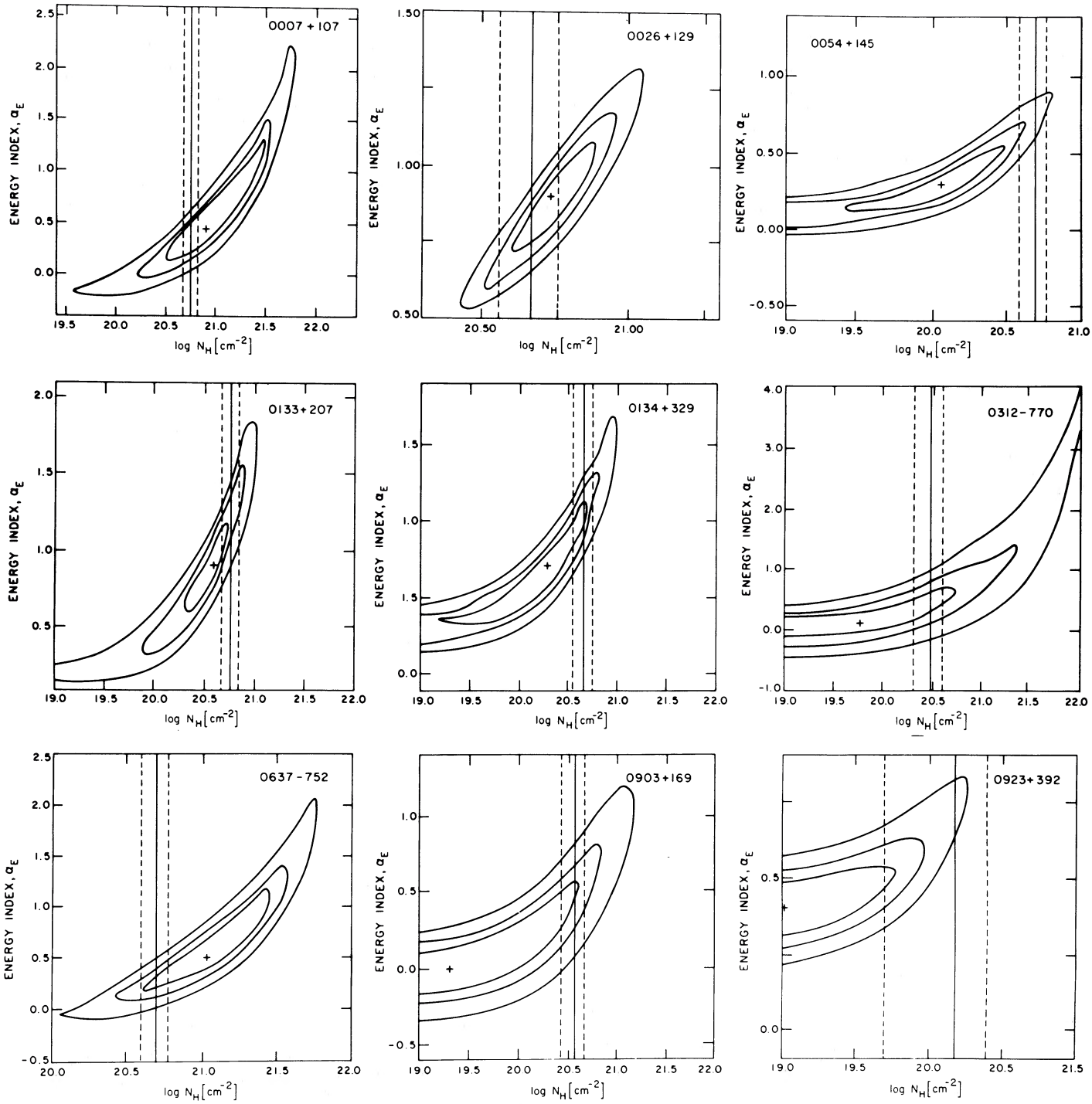

FIG. 2.—Two-dimensional χ^2 contours at 68%, 90%, and 99% confidence for all newly fitted quasars in order of right ascension. Galactic column determined from radio measurements (Stark *et al.* 1987) and estimated 90% error due to small-scale fluctuations are indicated.

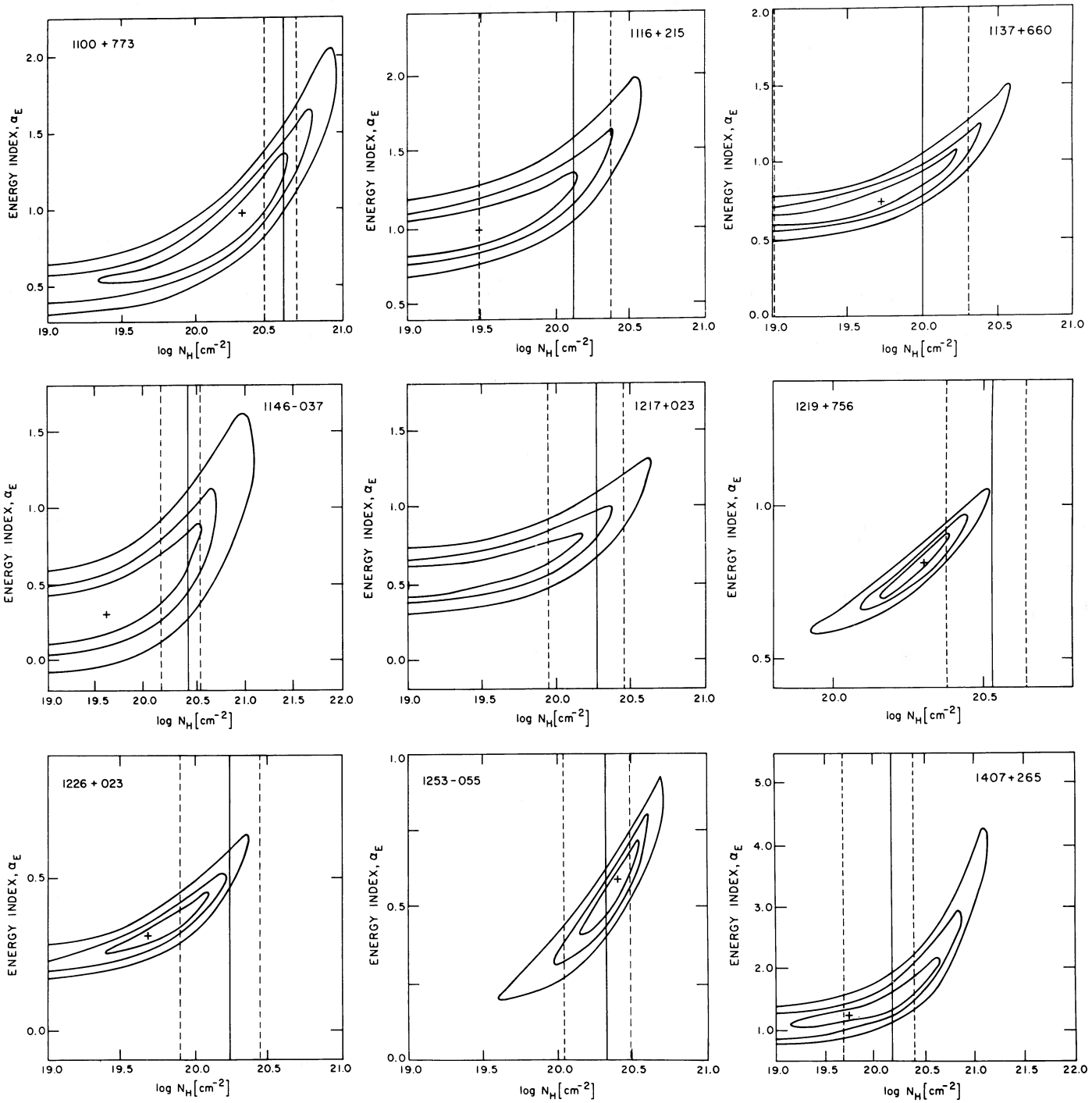

FIG. 2.—*Continued*

indices, the total sample includes 33 quasars. This sample is equivalent in size to that formed by combining all previous studies of emission-line AGNs that produced well-determined X-ray spectra. In addition, our sample covers a wider range of radio properties, redshift, and luminosity than did these earlier studies. We can now begin to investigate how the X-ray spectral index depends on other quasar properties.

a) Absorbing Column Density

Before discussing the spectral slopes of the quasars we find that there is an unexpected effect in the measurements of N_H which must be addressed. The X-ray measured column densities are correlated with the 21 cm Galactic column densities at better than 99.5% confidence (via a Spearman rank test). Thus, to first order, the IPC is measuring the absorbing column density through our Galaxy. There is no case in which N_H in excess of the 21 cm Galactic absorption is required by the X-ray data at $>90\%$ confidence. This implies a very clean line of sight down into the core of a number of quasars. However, when the sample of N_H measurements is considered as a whole, we find that the X-ray determined column densities are systematically low with respect to the 21 cm derived values.

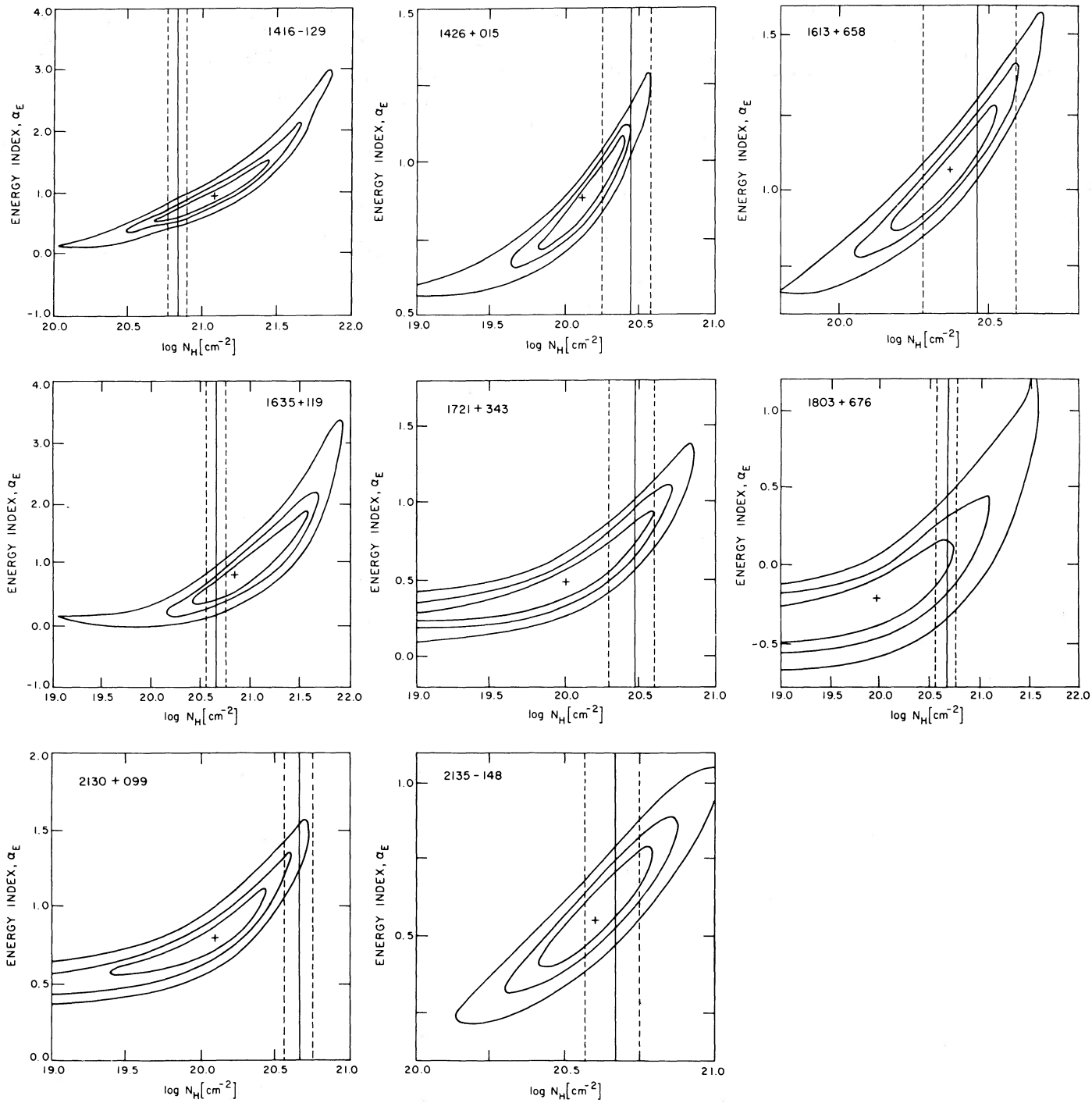

FIG. 2.—*Continued*

For seven quasars the X-ray derived N_H is smaller than the 21 cm value at >90% confidence (two-parameter) (footnoted in Table 3; see also Fig. 2).

In Figure 3*a* the distribution of $N_H(\mathrm{IPC}) - N_H(21\ \mathrm{cm})$ for the quasars is plotted. If all the quasars had a negligible intrinsic absorbing column, this distribution would be symmetric about zero with an approximately Gaussian distribution of a width consistent with the expected small-scale ($\sim 3'$) fluctuations in our Galaxy (Elvis *et al.* 1986, Appendix B) and the errors on the X-ray measurements. In contrast the distribution of $N_H(\mathrm{IPC}) - N_H(21\ \mathrm{cm})$ has a mean less than zero $[(-0.8 \pm 0.4) \times 10^{20}\ \mathrm{cm}^{-2}]$, a peak at $\sim -1.5 \times 10^{20}\ \mathrm{cm}^{-1}$, and only a small number of objects with $N_H(21\ \mathrm{cm}) < N_H(\mathrm{IPC})$. Figure 3*b* shows $N_H(\mathrm{IPC})$ versus $N_H(21\ \mathrm{cm})$ for those quasars with well-determined $N_H(\mathrm{IPC})$ (total error $\leq 7 \times 10^{20}\ \mathrm{cm}^{-2}$). The deficit in X-ray column persists over the full range of $N_H(21\ \mathrm{cm})$ and for a subset of quasars in which zero column density is excluded (*filled circles*). The observed distribution is different from that expected at >99% confidence (using a one-tail, K-S test). A χ^2 test, which includes allowance for errors on

TABLE 3

POWER-LAW FITS AND DERIVED FLUXES

Object	α_E	N_H (10^{20} atms cm^{-2})	χ^2_{min}/d.o.f.[a]	f(1 keV) μJy (observed)	f(0.3–3.5 keV) (10^{-11} erg cm^{-2} s^{-1}) (observed)	L_x(0.3–3.5 keV) (10^{45} erg s^{-1}) (at source)
0007+107 (III Zw 2)	$0.4^{+1.2}_{-0.4}$	$8.4^{+29.6}_{-6.5}$	7.2/8	$1.97^{+2.49}_{-0.52}$ ($1.67^{+0.48}_{-0.28}$)	$1.30^{+1.59}_{-0.19}$ ($1.09^{+0.06}_{-0.14}$)	$0.46^{+0.67}_{-0.08}$
0026+129 (PG)	$0.9^{+0.3}_{-0.3}$	$5.3^{+3.6}_{-1.9}$	8.3/7	$1.38^{+0.25}_{-0.17}$ ($1.25^{+0.14}_{-0.11}$)	$0.83^{+0.15}_{-0.08}$ ($0.69^{+0.03}_{-0.02}$)	$0.82^{+0.20}_{-0.11}$
0054+145[b] (PHL 909)	$0.3^{+0.4}_{-0.3}$	$1.1^{+2.7}_{-1.1}$	4.0/8	$0.47^{+0.11}_{-0.06}$ ($0.46^{+0.08}_{-0.05}$)	$0.32^{+0.03}_{-0.02}$ ($0.31^{+0.02}_{-0.02}$)	$0.43^{+0.07}_{-0.05}$
0133+207 (3C 47)	$0.9^{+0.7}_{-0.6}$	$3.5^{+4.2}_{-2.7}$	14.0/10	$0.82^{+0.25}_{-0.23}$ ($0.76^{+0.18}_{-0.20}$)	$0.48^{+0.19}_{-0.10}$ ($0.43^{+0.09}_{-0.09}$)	$5.30^{+4.18}_{-1.91}$
0134+329 (3C 48)	$0.7^{+0.6}_{-0.4}$	$1.9^{+4.0}_{-1.9}$	11.5/7	$0.50^{+0.14}_{-0.10}$ ($0.48^{+0.10}_{-0.08}$)	$0.31^{+0.08}_{-0.04}$ ($0.29^{+0.03}_{-0.02}$)	$2.29^{+1.19}_{-0.53}$
0205+024 (NAB)	$1.2^{+0.6}_{-0.1}$	$0.8^{+2.5}_{-0.3}$	8.2/7	$0.55^{+0.12}_{-0.03}$ ($0.55^{+0.08}_{-0.03}$)	$0.33^{+0.13}_{-0.02}$ ($0.32^{+0.05}_{-0.02}$)	$0.41^{+0.21}_{-0.03}$
0312−770 (PKS)	$0.1^{+1.3}_{-0.4}$	$0.6^{+19.5}_{-0.6}$	8.4/8	$0.49^{+0.59}_{-0.09}$ ($0.49^{+0.25}_{-0.09}$)	$0.36^{+0.30}_{-0.04}$ ($0.36^{+0.05}_{-0.05}$)	$0.79^{+1.10}_{-0.14}$
0637−752 (PKS)	$0.5^{+0.9}_{-0.4}$	$10.0^{+23.6}_{-7.3}$	2.6/7	$0.99^{+0.87}_{-0.26}$ ($0.82^{+0.16}_{-0.13}$)	$0.63^{+0.52}_{-0.09}$ ($0.51^{+0.03}_{-0.06}$)	$16.00^{+29.99}_{-4.79}$
0903+169 (3C 215)	$0.0^{+0.8}_{-0.2}$	$0.2^{+5.4}_{-0.2}$	2.1/8	$0.18^{+0.08}_{-0.02}$ ($0.18^{+0.06}_{-0.02}$)	$0.14^{+0.02}_{-0.01}$ ($0.14^{+0.02}_{-0.02}$)	$1.05^{+0.53}_{-0.14}$
0923+392[b] (4C 39.25)	$0.4^{+0.2}_{-0.2}$	$0.1^{+0.9}_{-0.1}$	19.8/8	$0.37^{+0.05}_{-0.02}$ ($0.37^{+0.04}_{-0.02}$)	$0.25^{+0.02}_{-0.01}$ ($0.24^{+0.03}_{-0.01}$)	$6.97^{+1.40}_{-0.95}$
1028+313 (B2)	$0.5^{+0.3}_{-0.1}$	$0.1^{+1.2}_{-0.1}$	2.5/6	$0.74^{+0.11}_{-0.04}$ ($0.74^{+0.09}_{-0.04}$)	$0.48^{+0.04}_{-0.02}$ ($0.47^{+0.03}_{-0.02}$)	$0.71^{+0.09}_{-0.04}$
1100+773 (3C 249.1)	$1.0^{+0.6}_{-0.6}$	$2.2^{+3.5}_{-2.2}$	9.4/8	$0.69^{+0.19}_{-0.13}$ ($0.66^{+0.13}_{-0.10}$)	$0.41^{+0.15}_{-0.04}$ ($0.38^{+0.04}_{-0.03}$)	$2.28^{+1.38}_{-0.53}$
1116+215 (PG)	$1.0^{+0.6}_{-0.2}$	$0.3^{+2.0}_{-0.3}$	2.6/7	$0.68^{+0.12}_{-0.06}$ ($0.68^{+0.09}_{-0.06}$)	$0.40^{+0.11}_{-0.04}$ ($0.40^{+0.05}_{-0.04}$)	$0.64^{+0.26}_{-0.08}$
1137+661 (3C 263)	$0.7^{+0.5}_{-0.2}$	$0.5^{+2.0}_{-0.5}$	14.5/8	$0.39^{+0.08}_{-0.02}$ ($0.39^{+0.05}_{-0.02}$)	$0.24^{+0.04}_{-0.01}$ ($0.24^{+0.06}_{-0.01}$)	$6.74^{+3.38}_{-0.90}$
1146−037 (PKS)	$0.3^{+0.8}_{-0.3}$	$0.4^{+5.2}_{-0.4}$	11.5/7	$0.56^{+0.26}_{-0.07}$ ($0.56^{+0.18}_{-0.07}$)	$0.38^{+0.12}_{-0.04}$ ($0.38^{+0.05}_{-0.04}$)	$2.12^{+1.63}_{-0.38}$
1202+281 (PG, GQ Comae)	$1.1^{+0.5}_{-0.5}$	$2.4^{+3.2}_{-2.4}$	5.3/6	$1.19^{+0.27}_{-0.25}$ ($1.14^{+0.16}_{-0.20}$)	$0.71^{+0.22}_{-0.13}$ ($0.64^{+0.06}_{-0.06}$)	$0.99^{+0.39}_{-0.24}$
1211+143 (PG)	$1.8^{+0.5}_{-0.4}$	$2.1^{+1.9}_{-1.3}$	14.6/7	$3.58^{+0.30}_{-0.33}$ ($3.43^{+0.18}_{-0.24}$)	$2.44^{+0.86}_{-0.44}$ ($2.12^{+0.30}_{-0.21}$)	$0.88^{+0.26}_{-0.18}$
1217+023 (PKS)	$0.5^{+0.5}_{-0.2}$	$0.1^{+2.3}_{-0.1}$	3.9/6	$1.11^{+0.27}_{-0.07}$ ($1.11^{+0.22}_{-0.07}$)	$0.71^{+0.12}_{-0.05}$ ($0.71^{+0.07}_{-0.05}$)	$1.98^{+0.60}_{-0.21}$
1219+756[b] (Mrk 205)	$0.8^{+0.2}_{-0.2}$	$2.0^{+0.9}_{-0.8}$	16.3/8	$2.24^{+0.15}_{-0.17}$ ($2.15^{+0.11}_{-0.13}$)	$1.35^{+0.08}_{-0.06}$ ($1.26^{+0.03}_{-0.03}$)	$0.30^{+0.02}_{-0.02}$
1226+023[b] (3C 273)	$0.3^{+0.2}_{-0.1}$	$0.6^{+1.0}_{-0.6}$	7.7/7	$10.98^{+1.14}_{-0.65}$ ($10.83^{+0.90}_{-0.53}$)	$7.49^{+0.26}_{-0.17}$ ($7.39^{+0.04}_{-0.08}$)	$8.45^{+0.55}_{-0.31}$
1253−055 (3C 279)	$0.6^{+0.2}_{-0.3}$	$2.6^{+1.8}_{-1.6}$	15.6/8	$0.64^{+0.07}_{-0.09}$ ($0.60^{+0.05}_{-0.06}$)	$0.40^{+0.03}_{-0.02}$ ($0.37^{+0.01}_{-0.02}$)	$6.76^{+1.16}_{-1.12}$
1307+085 (PG)	$0.9^{+0.7}_{-0.2}$	$0.3^{+2.2}_{-0.3}$	6.7/9	$0.81^{+0.12}_{-0.06}$ ($0.80^{+0.10}_{-0.06}$)	$0.48^{+0.12}_{-0.03}$ ($0.48^{+0.05}_{-0.03}$)	$0.59^{+0.25}_{-0.05}$
1407+265 (PG)	$1.2^{+1.7}_{-0.4}$	$0.5^{+6.7}_{-0.5}$	3.3/7	$0.44^{+0.17}_{-0.05}$ ($0.44^{+0.09}_{-0.05}$)	$0.26^{+0.48}_{-0.03}$ ($0.26^{+0.13}_{-0.03}$)	$24.69^{+192.91}_{-7.95}$
1416−129 (PG)	$0.9^{+1.3}_{-0.6}$	$11.9^{+39.4}_{-9.1}$	12.0/8	$2.15^{+3.50}_{-0.70}$ ($1.71^{+0.39}_{-0.34}$)	$1.30^{+3.36}_{-0.29}$ ($0.92^{+0.05}_{-0.12}$)	$1.03^{+3.34}_{-0.29}$
1426+015[b] (PG)	$0.9^{+0.2}_{-0.2}$	$1.3^{+1.4}_{-0.7}$	12.8/6	$1.67^{+0.23}_{-0.10}$ ($1.62^{+0.17}_{-0.16}$)	$0.99^{+0.05}_{-0.05}$ ($0.94^{+0.05}_{-0.05}$)	$0.34^{+0.02}_{-0.02}$
1501+106[b] (PG, Mrk 841)	$1.0^{+0.4}_{-0.4}$	$1.2^{+1.2}_{-1.1}$	2.8/8	$4.15^{+0.24}_{-0.37}$ ($4.06^{+0.18}_{-0.29}$)	$2.47^{+0.21}_{-0.13}$ ($2.35^{+0.10}_{-0.09}$)	$0.14^{+0.02}_{-0.01}$
1545+210 (PG, 3C 323.1)	$0.8^{+0.6}_{-0.7}$	$3.2^{+6.8}_{-3.2}$	7.4/7	$1.10^{+0.43}_{-0.29}$ ($1.03^{+0.25}_{-0.22}$)	$0.66^{+0.28}_{-0.07}$ ($0.60^{+0.04}_{-0.04}$)	$2.46^{+1.58}_{-0.59}$
1613+658 (PG)	$1.1^{+0.3}_{-0.3}$	$2.4^{+1.6}_{-1.4}$	7.0/9	$1.31^{+0.17}_{-0.17}$ ($1.25^{+0.12}_{-0.13}$)	$0.78^{+0.12}_{-0.09}$ ($0.70^{+0.05}_{-0.04}$)	$0.64^{+0.13}_{-0.09}$

TABLE 3—*Continued*

Object	α_E	N_H (10^{20} atms cm^{-2})	χ^2_{min}/d.o.f.[a]	f(1 keV) μJy (observed)	f(0.3–3.5 keV) (10^{-11} erg cm^{-2} s^{-1}) (observed)	L_x(0.3–3.5 keV) (10^{45} erg s^{-1}) (at source)
1635+119	$0.9^{+1.4}_{-0.7}$	$5.9^{+29.6}_{-5.2}$	12.5/8	$0.38^{+0.54}_{-0.11}$ ($0.34^{+0.12}_{-0.08}$)	$0.23^{+0.56}_{-0.04}$ ($0.19^{+0.01}_{-0.02}$)	$0.24^{+0.46}_{-0.06}$
1721+343 (4C 34.47)	$0.5^{+0.6}_{-0.3}$	$1.0^{+4.2}_{-1.0}$	5.1/9	$1.93^{+0.73}_{-0.20}$ ($1.90^{+0.51}_{-0.17}$)	$1.24^{+0.35}_{-0.07}$ ($1.20^{+0.12}_{-0.07}$)	$2.51^{+1.09}_{-0.27}$
1803+676 (KAZ 102)	$0.2^{+0.6}_{-0.4}$	$0.9^{+12.6}_{-0.9}$	6.7/9	$0.33^{+0.20}_{-0.06}$ ($0.33^{+0.08}_{-0.06}$)	$0.29^{+0.06}_{-0.02}$ ($0.28^{+0.03}_{-0.02}$)	$0.23^{+0.06}_{-0.03}$
2130+099[b] (PG, II Zw 136)	$0.8^{+0.6}_{-0.4}$	$1.2^{+2.6}_{-1.2}$	6.2/8	$0.69^{+0.15}_{-0.07}$ ($0.68^{+0.10}_{-0.07}$)	$0.42^{+0.09}_{-0.03}$ ($0.40^{+0.03}_{-0.02}$)	$0.07^{+0.02}_{-0.00}$
2135−148 (PHL 1657)	$0.5^{+0.4}_{-0.2}$	$3.8^{+3.9}_{-1.7}$	20.7/8	$1.01^{+0.13}_{-0.12}$ ($0.94^{+0.12}_{-0.09}$)	$0.65^{+0.09}_{-0.05}$ ($0.59^{+0.02}_{-0.02}$)	$1.24^{+0.27}_{-0.14}$

[a] Degrees of Freedom.
[b] Quasars for which the X-ray N_H is less than the 21 cm measurement for our Galaxy at >90% confidence.

N_H treated as the only interesting parameter, confirms the result at $>50\ \sigma$. Omitting the two most extreme objects, 0923+392 and 1028+313, it is a 15 σ effect, still highly significant.

The first possible explanation to be considered is selection. Our sample is not well defined and the distribution may be biased due to our inability to fit objects with high absorbing columns. The maximum total absorbing column for which a good spectral fit can be made is a complicated function of the quasar spectral slope and redshift, the signal-to-noise ratio of the data and the instrument gain. An investigation using simulated data is underway from which we aim to define the parameter space in which we can work. However, if our sample is limited by an inability to fit at high column densities we might expect one of the following two effects:

1. At low Galactic column densities we would expect to find X-ray column densities distributed evenly about the Galactic value. As the Galactic column increases beyond an upper limit, the spectral slope becomes ill determined and would be dropped from our sample. We would then preferentially select objects with lower X-ray columns, which remain below this limit. No such selection is observed, it is apparent from Figure 3*b* that the N_H deficit occurs at all Galactic columns.

2. Perhaps the strongest argument can be made by considering a sample chosen by the signal-to-noise ratio of the source detection. Such a sample should not show any N_H deficit since no objects are excluded due to poor α_E and N_H constraints. Our sample is complete for S/N ratio >25. This subsample of 22 quasars has an X-ray N_H distribution which is different from that of the Galaxy at $>50\ \sigma$ confidence (using a χ^2 test with N_H as the only interesting parameter).

We thus consider it unlikely that the observed N_H deficit is a result of sample selection.

The cause of the N_H deficit could lie in any of several places: the IPC calibration may be in error; the local interstellar medium of our Galaxy could be peculiar in its small-scale structure or its abundances; or the quasar spectra may have an upturn in the very lowest part of the IPC energy range. We believe this last possibility is the correct one. Peculiarities in the interstellar medium are implausible. Many authors have argued against the existence of large amplitude H I structure on a scale smaller than several arcminutes (see Lockman, Hobbs, and Shull 1986, and references therein). Without such structure to allow clean lines of sight to quasars the only degree of freedom remaining is the abundances.[1] Soft X-rays at 0.2 keV are primarily absorbed by helium (Morrison and McCammon 1983). To produce the observed deficit, the helium abundance in the local interstellar medium would need to be roughly half what it is believed to be—at best an unlikely possibility (Pagel 1982), although we note that it is not yet directly measured (e.g., through He Lyα absorption, using EUVE or Lyman/FUSE; Bowyer 1986).

The simplest test for whether the cause of the deficit is intrinsic to the quasars or not is to find a sample of X-ray point sources beyond the H I layer of the Galactic plane that were observed on-axis by the IPC, as were the quasars. Such samples are not common. However G. Madejski has pointed out to us that some BL Lac objects observed with *Einstein* do have the necessary properties. Figures 4*a* and 4*b* compare the 21 cm and X-ray N_H values for the 11 BL Lac objects with well-constrained N_H from Madejski (1985). The agreement is excellent. There is no tendency for the X-ray measured columns to be low as there is in the quasars (compare Figs. 3 and 4).

Thus the N_H deficit in the quasars cannot be due to instrument calibration or to peculiar Galactic absorption since this would affect BL Lac objects and quasars alike. We conclude that, instead, the quasar emission spectra must have an excess below ~0.3 keV. The only BL Lac object with a clear N_H deficit is PKS 2155−305 which is known to have an ultrasoft excess (Canizares and Kruper 1984). BL Lac objects have been described as having "soft excess" spectra below ~2 keV for several years (Agrawal, Riegler, and Mushotzky 1979; Urry, Mushotzky, and Holt 1986). However, the quasar excesses lie almost a decade lower in energy (~0.2 keV), and so we will call them "ultrasoft excesses."

The amplitude of the ultrasoft excesses is ~60% above the single power law 0.2 keV flux density after absorption by Galactic N_H. No correlation was found between the N_H deficit and redshift (correlation coefficient 0.07) or the ratio L_{opt}/L_x (correlation coefficient −0.15), implying a remarkably constant ultrasoft excess over a wide range in both parameters (see Table 1). An exception may be PG 1211+143 (see § III*b*). Similar ultrasoft excesses have been found in a number of

[1] We also note that the relevant atomic cross sections are measured to about 1% (Berrington *et al.* 1982), and so errors in these values are too small to cause the present discrepancy.

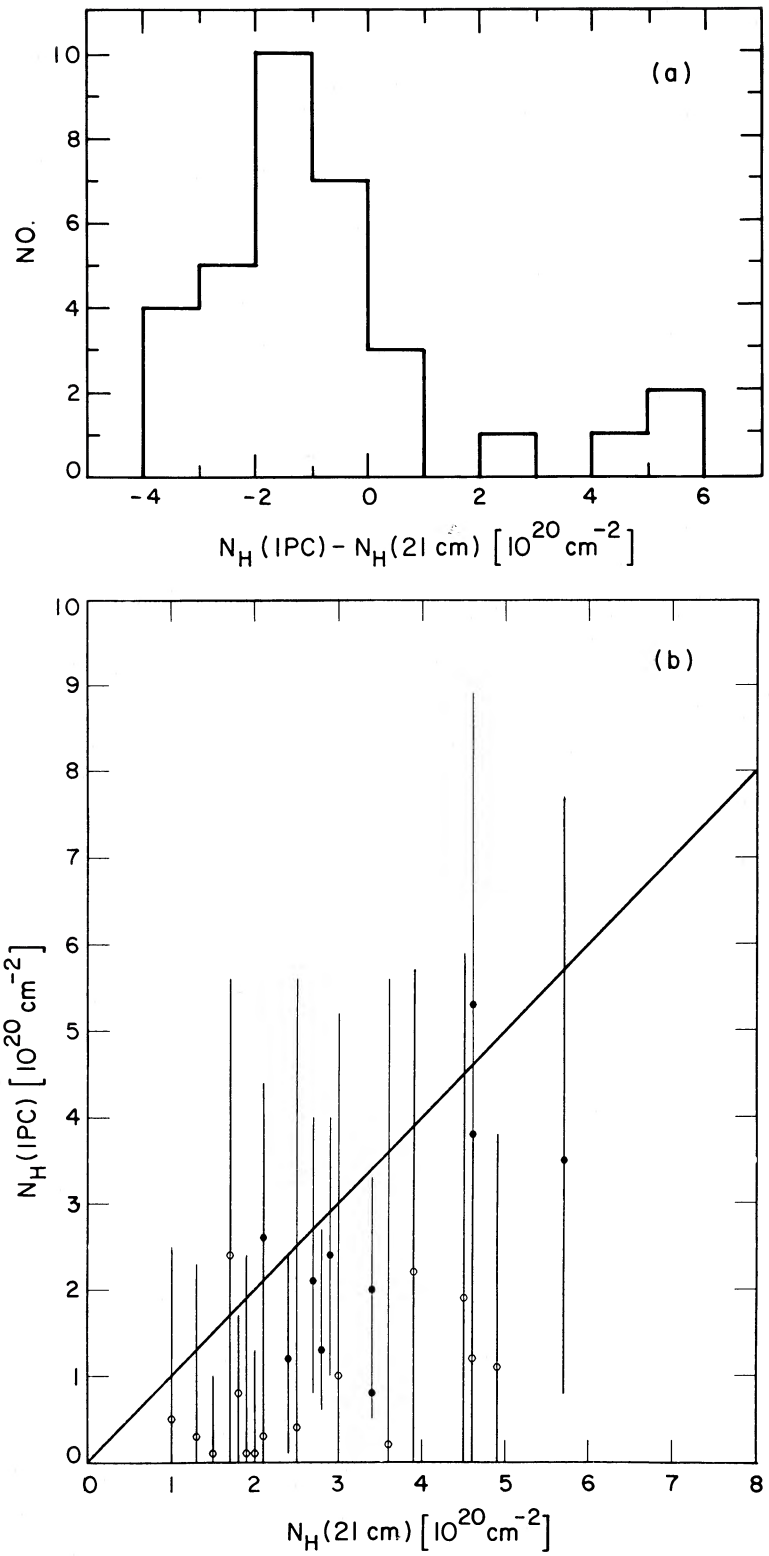

FIG. 3.—(*a*) Distribution of difference between the X-ray best estimate of the Galactic absorbing column density (N_H[IPC]) and the radio measured value (N_H[21 cm]) in units of 10^{20} cm^{-2}. (*b*) X-ray absorbing column density vs. radio absorbing column density for those objects with total (90% confidence) error in N_H(IPC) $< 7 \times 10^{20}$ cm^{-2}. Solid line indicates equality. X-ray estimated columns not consistent with zero (at 90% confidence) are shown as filled circles. The 90% error in N_H(21 cm) ($\pm 1 \times 10^{20}$ cm^{-2}) is not indicated to avoid confusion.

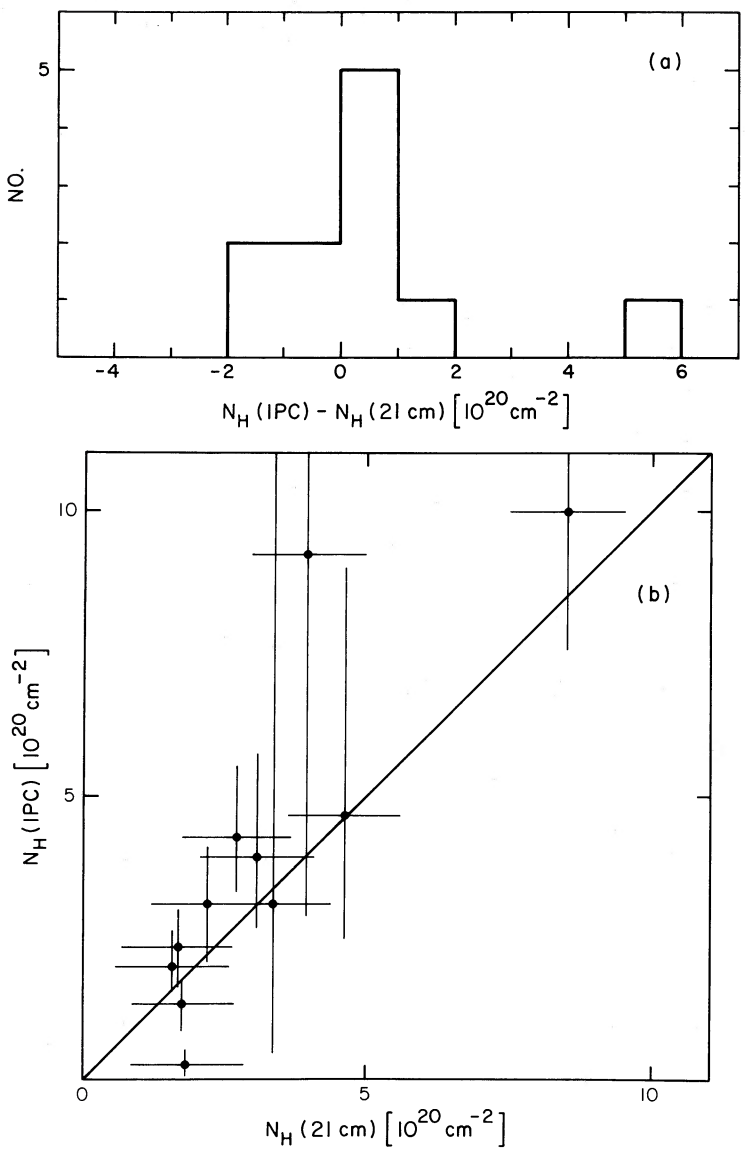

FIG. 4.—(*a*) and (*b*) as in Fig. 3 but for the BL Lac sample of Madejski (1985)

AGNs with the *EXOSAT* Channel Multiplier Array (CMA) (Arnaud *et al.* 1985; Pounds *et al.* 1986). The CMA is sensitive to even lower energies than the IPC. Branduardi-Raymont *et al.* (1986) also present evidence for ultrasoft excesses based on the detection in a CMA deep survey of many more AGNs than expected from number counts at higher energies. Their lack of detection of a number of high-redshift quasars also present in the same field (Hoag, Thomas, and Vaucher 1982) may imply that these excesses fall steeply to higher energies. They also vary strongly on a time scale of 1 yr (Branduardi-Raymont *et al.* 1987).

It is interesting that ultrasoft excesses are not often seen in BL Lac objects. The most notable differences between BL Lac objects and quasars are the lack of an optical-UV "big blue bump" and the lack of broad emission lines in the BL Lac objects. The presence of an ultrasoft excess in quasars and not in BL Lac objects supports earlier suggestions (e.g., Bechtold *et al.* 1986) that the excess is the high-energy tail of the big blue bump. This picture is also consistent with the presence of broad emission lines in quasars. The emission lines originate in gas photoionized by the UV and soft X-ray photons which would dominate the energy output of quasars while being far less prominent in BL Lac objects.

The IPC alone does not have sufficient spectral coverage or resolution to define the ultrasoft excesses more precisely through two-component model fits. In order to study them we are obtaining more accurate 21 cm Galactic column densities and investigating the use of higher energy monitor proportional counter (MPC) data to determine the higher energy slope better. This analysis will be reported in a later paper.

b) X-Ray Spectral Indices

The most striking result of our survey is the large range of energy spectral index, α_E, present in the sample. In Figure 5 a double histogram of the best fit α_E is displayed. Radio-loud objects (see § III*d*) are shown with a solid line, and radio-quiet with a dotted line. The full range of slopes is wide with extreme values of -0.2 and 1.8. The radio-loud quasars cluster around

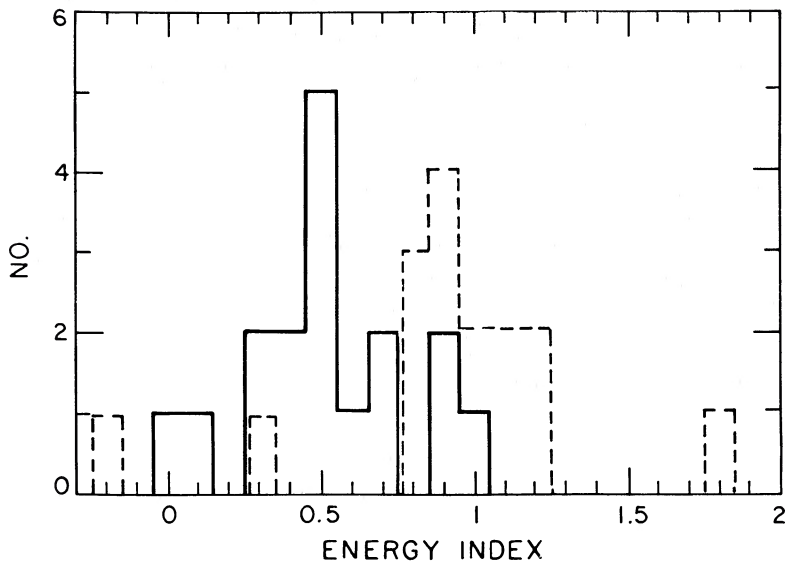

FIG. 5.—Double histogram showing distribution of X-ray slope (α_E) for radio-loud (*solid line*) and radio-quiet (*dotted line*) quasars

$\alpha_E = 0.5$, while the radio-quiet quasars are grouped around $\alpha_E = 1.0$ (see § III*d*, below).

There are two extreme objects: one at either end of the distribution. The steepest spectrum is that of PG 1211+143 ($\alpha_E = 1.8$, see Table 3). This object is discussed in detail by Bechtold *et al.* (1986) in terms of a two–power-law fit to the IPC combined with the higher energy MPC data. The steep low-energy component may be an ultrasoft excess, as discussed in the previous section, but one extending to higher energies than in most quasars. No other examples of steep "PG 1211+143–like" spectra have appeared in our sample, implying that they must either be rather rare or strongly selected against.

The other extreme object is 1803+676 for which the best-fit spectrum is inverted, setting it apart from the rest of the objects. The 90% confidence errors allow a slope as steep as 0.4 (Table 2), which is still unusually flat for a radio-quiet quasar such as this (see § III*c*). Its special status as both, radio-quiet and with a flat X-ray spectrum makes it valuable as a diagnostic in emission-line studies (Wilkes, Elvis, and McHardy 1987).

c) Spectral Dependence of Flux Density Measurements

The 2 keV monochromatic luminosity, $L_{2\,\mathrm{keV}}$, of quasars has been widely used in estimating the contributions of the evolving quasar population to the diffuse X-ray background (e.g., Schmidt and Green 1986; Avni and Tananbaum 1986). With present instrumentation, an assumption of spectral shape is needed to derive $L_{2\,\mathrm{keV}}$. In Figure 6 we compare on a log scale our estimate of $L_{2\,\mathrm{keV}}$, using the IPC spectral result for α_E and N_H, with those of Tananbaum *et al.* (1986) and Tananbaum *et al.* (1983), who assumed $\alpha = 0.5$ and Galactic N_H, as a function of α_E. When our study used different observations from those used in the earlier study, the derived fluxes were normalized to the same count rate to effect a proper compari-

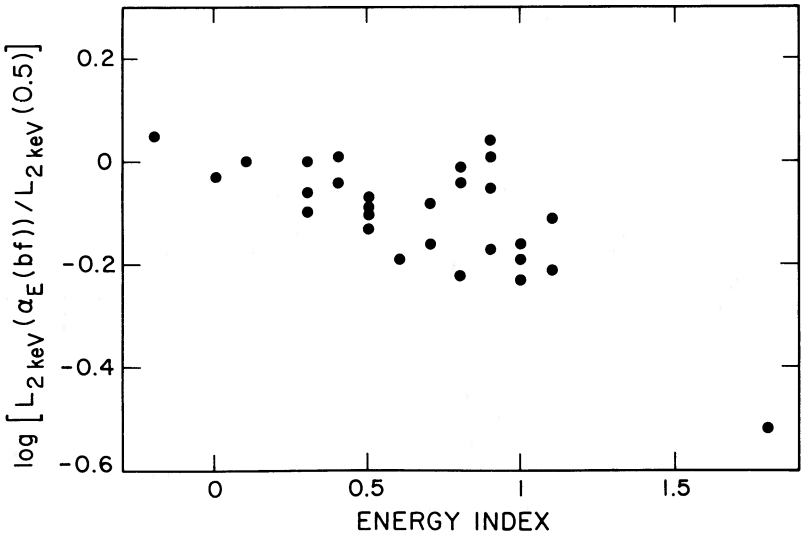

FIG. 6.—Logarithm of the ratio of 2 keV luminosities, $L_{2\,\mathrm{keV}}$ (α_E[best-fit]) from our study to those from earlier studies $L_{2\,\mathrm{keV}}(0.5)$ as a function of α_E. In this paper the 2 keV luminosities were determined using the best-fit α_E and N_H for each quasar. Earlier studies assumed $\alpha_E = 0.5$ and Galactic N_H from radio measurements.

son of the two data sets. As expected (Elvis *et al.* 1986), there is a clear trend toward lower $L_{2\,\mathrm{keV}}$ for larger α_E. (The offset at $\alpha_E = 0.5$ is due to our use of an updated effective area table for the IPC; Harnden *et al.* 1984.) The larger scatter in the points at large α_E reflects the greater influence of N_{H} in determining $L_{2\,\mathrm{keV}}$ for steep-spectrum objects.

Since most quasars are radio-quiet and so likely to have steeper soft X-ray slopes, this change of derived flux with X-ray slope will be important in estimating the contribution of quasars to the diffuse X-ray background. The dependence of $f_{2\,\mathrm{keV}}$ on α_E also introduces an interdependence of α_E and α_{ox}, which is defined using $f_{2\,\mathrm{keV}}$. To avoid this complication, the ratio of optical to broad-band X-ray luminosity (L_{opt}/L_x), which is much less sensitive to changes in α_E, will be used instead of α_{ox} in this paper.

d) X-Ray Spectral Index and Radio Loudness

As we have seen in Figure 5, there is a clear trend for radio-quiet quasars to have steeper X-ray spectra than radio-loud quasars. (We define radio loud as having $R_L(= \log (f_R/f_B) > 1$ in Table 4; see below.) There is convincing evidence in the literature that the radio properties of quasars are closely related to their X-ray luminosity. Zamorani *et al.* (1981) and Worrall *et al.* (1987) have shown that radio-loud quasars are relatively more luminous in X-rays and have suggested that they possess an additional X-ray production mechanism linked to the radio emission such as synchrotron or synchrotron self-Compton (Kembhavi 1985). A very strong link between 90 GHz and X-ray emission was found for strong millimeter sources by Owen, Helfand, and Spangler (1981). Since the dominant X-ray production mechanism may be different depending upon a quasar's radio luminosity, we might also expect the X-ray slope to be different.

We have collected published 5 GHz radio core fluxes for all the quasars in our sample (Table 4). The fluxes for the PG quasars were kindly supplied by K. Kellerman in advance of publication (Kellerman *et al.* 1987). We have selected, as far as possible, observations taken with the same projected physical beam size, typically a few tens of kiloparsecs (Table 4, column 4). When the beam sizes do not match it is usually because the radio-loud quasars were observed at the highest VLA resolution. Any correction to a larger beam could only make these objects more radio loud. Three southern quasars, having only Parkes survey fluxes, are exceptions to this rule. For optical fluxes we used B magnitudes converted to millijanskys on the Johnson (1966) scale. No attempt was made to correct

TABLE 4

RADIO AND OPTICAL DATA FOR QUASARS WITH IPC X-RAY SPECTRA

Object	f_R (5 GHz, mJy)	HPBW (arcsec)	HPBW (kpc)	References for Radio Data	f_B[a] (mJy)	R_L	log L_{opt}[b]
0007+107	320.	18	41.0	1	1.84	2.24	29.69
0026+129	5.1	18	61.0	1	2.33	0.34	30.21
0054+145	1.0 ± 0.2	10	39.4	2	1.02	−0.01	30.02
0133+207	80 ± 10	8	14.8	3	0.24	2.52	30.23
0134+329	5600	2	13.5	4	1.41	3.60	30.86
0205+024	0.9 ± 15	13	47.3	5	2.25	−0.40	30.27
0312−770	5600 ± 30	237	1142	6	1.39	3.61	30.39
0637−752	5490	237	2181	7	1.64	3.52	31.48
0903+169	20 ± 10	2	14.5	3	0.18	2.05	30.07
0923+392	7600	0.4	3.8	8	0.30	4.40	30.81
1028+313	91	4	16.2	9	0.66	2.14	29.86
1100+773	110 ± 20	2	12.2	3	2.33	1.82	30.92
1116+215	2.8	18	72.8	1	3.80	−0.13	30.62
1137+661	130	2	18.4	3	1.12	2.06	31.32
1146−037	290	240	1548.5	10	0.73	2.60	30.51
1202+281	0.83	18	68.9	1	2.33	−0.45	30.34
1211+143	1.2	18	39.4	1	6.25	−0.72	30.18
1217+023	257	10	50.8	11	1.07	2.38	30.35
1219+756	1.2	5.3	9.7	2	2.47	−0.31	29.60
1226+023	30500	0.4	1.5	8	26.30	3.06	31.36
1253−055	9500	0.4	3.4	8	0.28	4.53	30.53
1307+085	0.35	18	65.5	1	3.44	−0.99	30.45
1407+265	6.2	18	192.4	1	2.27	0.44	32.00
1416−129	3.6	18	56.4	1	3.08	0.07	30.24
1426+015	1.21	18	39.8	1	4.25	−0.55	30.02
1501+106	1.5 ± 0.25	18	17.9	1	7.05	−0.67	29.47
1545+210	<1	0.4	2.2	12	0.85	<0.07	30.34
1613+658	3.03	18	56.4	1	2.42	−0.10	30.14
1635+119	18	4	13.9	9	0.72	1.40	29.72
1721+343	370	0.4	1.8	12	1.10[c]	2.53[c]	30.17
1803+676	<0.35	0.4	1.3	13	1.71	<0.69	30.03
2130+099	2.05	18	29.2	1	4.79	0.37	29.77
2135−148	126	0.4	1.8	12	2.49	1.70	30.55

[a] Calculated from m_B using $m_B(\phi) = 4440$ Jy; Johnson 1966.

[b] Calculated for ($H_0 = 50\,\mathrm{km\,s^{-1}\,Mpc^{-1}}$, $q_0 = 0, \alpha = 0.5$).

[c] As no B magnitude is available, f_V is used.

REFERENCES.—(1) Kellerman *et al.* 1987; (2) Gioia 1986; (3) Pooley and Henbest 1974; (4) Elsmore and Ryle 1976; (5) Rudnick, Sitko, and Stein 1984; (6) Shimmins and Bolton 1972; (7) Savage 1976; (8) Perley 1982; (9) Feigelson, Isobe, and Kembhavi 1984; (10) Wall 1972; (11) Neff and Browne 1984; (12) Gower and Hutchings 1984; (13) Hutchings and Gower 1985.

for line emission since unavoidable errors due to uncertain spectral slope and Galactic absorption are at least comparable and the line equivalent widths are not well known. The ratio of 5 GHz radio core flux density to flux density at B, log (f_R/f_B), forms an index of radio loudness, R_L. With this index we can now treat radio loudness as a continuous variable. Also given in Table 4 is log $L_{\rm opt}$ defined at 2500 Å. It is derived from L_B assuming $\alpha_E = 0.5$ in the optical-UV region.

In Figure 7 radio loudness, R_L, is plotted as a function of X-ray spectral index, α_E. Again there is a clear tendency for radio-loud quasars to have flatter slopes; the correlation is significant at >99% confidence (using a Spearman rank test). The sample divides cleanly into radio-loud and radio-quiet at $R_L \sim 1$ (i.e., effective radio to optical slope, $\alpha_{ro} \sim 0.2$) with only two quasars (and one upper limit) in the range $0.5 \leq R_L \leq 1.5$. This scarcity of intermediate R_L quasars makes it difficult to distinguish between a continuous change of α_E with R_L and two separate classes of object having $\alpha_E \approx 0.5$ and 1.0, respectively. It is notable that two quasars clearly do not follow the correlation: 1803+676 and PHL 909 (Fig. 7).

In our sample those quasars with high radio luminosity are also those with high X-ray luminosity, low optical to X-ray luminosity ratio $(L_{\rm opt}/L_x)$ and high redshift. Any of these variables—radio loudness, X-ray luminosity, $L_{\rm opt}/L_x$, optical luminosity, or redshift—could be the controlling variable that determines the X-ray spectral slope. In the case of redshift this change of slope could simply be the redshifting of a soft excess out of the low-energy carbon window in the IPC response. Figures 8*a*, 8*b*, 8*c*, and 8*d* show redshift (z), X-ray luminosity (L_x), $L_{\rm opt}/L_x$, and optical luminosity ($L_{\rm opt}$), respectively, plotted as a function of X-ray energy index, α_E. In order to determine the fundamental correlation and to allow for the interdependence of the six variables, we performed a nonparametric partial Spearman rank correlation analysis. Table 5 gives the t-values[2] and corresponding probabilities of a correlation for each pair of variables with the other four held constant. Luminosity and redshift are inevitably tightly linked. Allowing for this, the only significant correlation is that of X-ray slope, α_E, with radio loudness, R_L. We conclude that this is the primary relation.

[2] The t-value $t = r_S(N - 2/1 - r_S^2)^{1/2}$, where r_S = Spearman rank correlation coefficient; t is distributed according to the Student's t-statistic with $N - 2$ degrees of freedom.

TABLE 5

RESULTS OF PARTIAL SPEARMAN RANK CORRELATION[a]

Variables Correlated	Variable Held Constant	t	P[b]
α_E, R_L	$L_x, z, L_{\rm opt}/L_x, L_{\rm opt}$	−3.98	<0.005
α_E, L_x	$R_L, z, L_{\rm opt}/L_x, L_{\rm opt}$	0.98	0.180
α_E, z	$R_L, L_x, L_{\rm opt}/L_x, L_{\rm opt}$	−0.41	0.344
$\alpha_E, L_{\rm opt}/L_x$	$R_L, L_x, z, L_{\rm opt}$	0.48	0.320
$\alpha_E, L_{\rm opt}$	$R_L, L_x, z, L_{\rm opt}/L_x$	−0.00	>0.400
R_L, L_x	$\alpha_E, L_{\rm opt}/L_x, z, L_{\rm opt}$	0.90	0.200
R_L, z	$\alpha_E, L_{\rm opt}/L_x, L_x, L_{\rm opt}$	1.24	0.120
$R_L, L_{\rm opt}/L_x$	$\alpha_E, z, L_x, L_{\rm opt}$	−0.55	0.293
$R_L, L_{\rm opt}$	$\alpha_E, z, L_x, L_{\rm opt}/L_x$	−0.07	>0.400
L_x, z	$\alpha_E, R_L, L_{\rm opt}/L_x, L_{\rm opt}$	1.12	0.146
$L_x, L_{\rm opt}/L_x$	$\alpha_E, R_L, z, L_{\rm opt}$	−5.80	<0.005
$L_x, L_{\rm opt}$	$\alpha_E, R_L, z, L_{\rm opt}/L_x$	7.31	<0.005
$z, L_{\rm opt}/L_x$	$\alpha_E, R_L, L_x, L_{\rm opt}$	−0.13	>0.400
$z, L_{\rm opt}$	$\alpha_E, R_L, L_x, L_{\rm opt}/L_x$	0.94	0.190
$L_{\rm opt}, L_{\rm opt}/L_x$	α_E, R_L, L_x, z	7.80	<0.005

[a] Six variables: $R_L, \alpha_E, L_x, z, L_{\rm opt}/L_x, L_{\rm opt}$.
[b] One-tailed probabilities for 33 objects.

e) *Comparison with Previous Results*

There are previous X-ray spectral studies with which we can compare our results. In particular, there is the derivation of a "mean spectral slope" for 25 quasars (Worrall and Marshall 1984) and the studies of individual AGNs by *HEAO 1* A-2 (Mushotzky 1984) and *Einstein* SSS (Petre *et al.* 1984).

The dependence of X-ray spectral index, α_E, on radio loudness, R_L, can explain the result of Worrall and Marshall (1984) that the weighted mean slope of a sample of 25 quasars over the ~1–6 keV range was 0.83(+0.32, −0.22). Their sample contained 19 radio-loud and six radio-quiet quasars but was dominated by four objects only one of which was radio loud. The mean slope expected from these four, assuming radio-loud quasars have $\alpha_E = 0.5$ and radio-quiet quasars have $\alpha_E = 1.0$, is 0.88, close to the value actually found.

Less easy to understand is the strong preference of AGNs

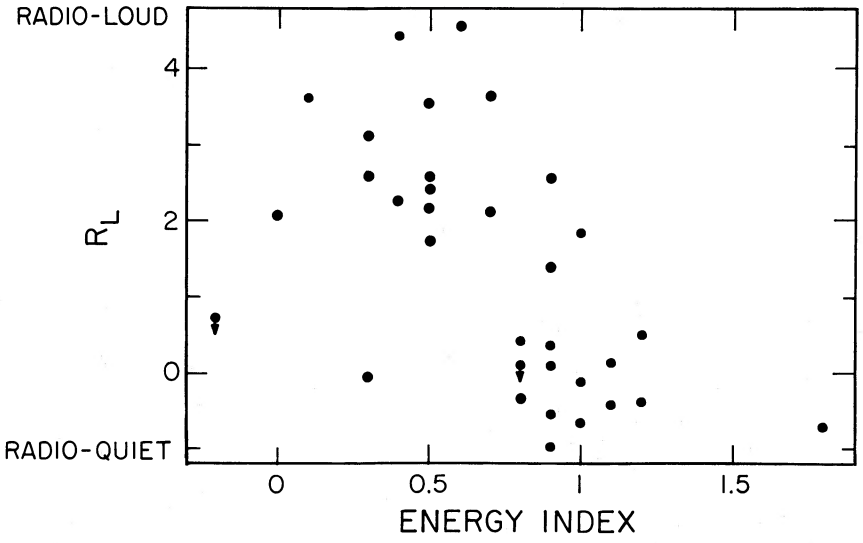

FIG. 7.—Radio loudness (R_L) as a function of X-ray slope, α_E, for IPC quasar sample

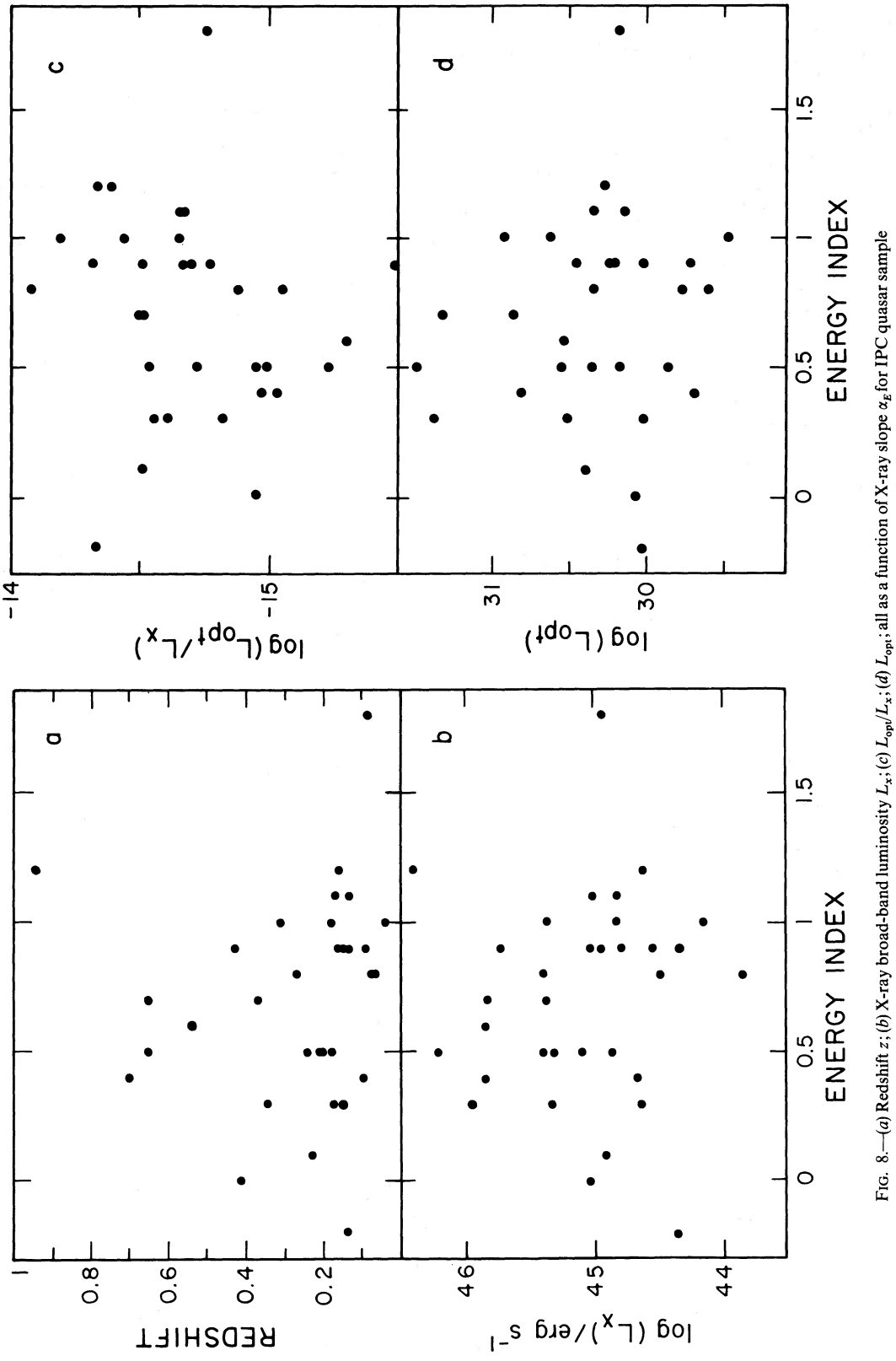

FIG. 8.—(*a*) Redshift z; (*b*) X-ray broad-band luminosity L_x; (*c*) L_{opt}/L_x; (*d*) L_{opt}; all as a function of X-ray slope α_E for IPC quasar sample

TABLE 6

RADIO LOUDNESS AND X-RAY SLOPE FOR AGNs WITH SSS AND A-2 SPECTRA[a]

Object	f_B (mJy)	References for f_B	f_R (mJy)	References for f_R	R_L	α_E(SSS)[b]	α_E(A-2)[c]
0003+199 (Mrk 335)	14.0	1	<40	3	<0.5	...	0.78 ± 0.2
0007+106 (III Zw 2)	3.8	1	184	4	1.7	$0.67^{+0.5}_{-0.4}$	...
0120−591 (F9)	16.0	1	<9	4	<−0.25	0.84 ± 0.35[d]	...
0206−019 (Mrk 590)	8.4	1	3.5	4	−0.4	...	0.63 ± 0.3
0432+05 (3C 120)	2.2	1	2254	4	3.0	...	$0.72^{+0.23}_{-0.05}$
1135−373 (NGC 3783)	7.8	1	13	4	0.2	...	0.59 ± 0.17
1226+022 (3C 273)	26.4	1	30500	4	3.1	0.44 ± 0.15[d]	0.41 ± 0.02
1359+69 (Mrk 279)	3.5	2	7.7	5	0.3	...	0.88 ± 0.20
1353+38 (Mrk 464)	0.7	2	5.8	5	0.9	...	0.40 ± 0.15
1415+255 (NGC 5548)	11.0	1	8	4	−0.1	...	0.68 ± 0.11
1845+78 (3C 390.3)	0.81	1	400	6	2.7	...	$0.65^{+0.50}_{-0.25}$
1914−589 (ESO 141−G55)	8.1	1	<12	4	<0.18	1.4 ± 0.4	...
2040−115 (Mrk 509)	11.8	1	4.5	4	−0.4	0.94 ± 0.5	0.63 ± 0.10
2259+085 (NGC 7469)	12.8	1	65	4	0.7	0.89 ± 0.3	0.78 ± 0.2
2302−088 (MCG−2-58-22)	6.6	1	9	4	0.1	0.54 ± 3	0.55 ± 0.05

[a] Includes only objects with (1) $(U-B) < -0.44$, i.e., those which qualify for the PG sample based on their color and (2) $\Delta\alpha_E$ (total) ≤ 0.9.

[b] From Petre *et al.* 1984.

[c] From Mushotzky 1984.

[d] Mean of reported values.

REFERENCES.—(1) McAlary *et al.* 1983; (2) Véron-Cetty and Véron 1983; (3) Sramek and Tovmassian 1975; (4) Unger *et al.* 1987; (5) Ulvestad and Wilson 1984; (6) Hargrave and McEllin 1975.

measured by *HEAO 1* A-2 (Mushotzky 1984) and by the *Einstein* SSS (Petre *et al.* 1984) to have $\alpha_E = 0.7$, with small dispersion. The $\alpha_E = 0.7$ rule seems to apply regardless of radio loudness since several Third Cambridge catalog (3C) radio galaxies have been measured by each instrument. There is now good radio data available for most of the objects in the *HEAO 1* A-2 and SSS samples (Unger *et al.* 1987), and we have constructed R_L for them in the same way as for our sample. We have restricted ourselves to those objects in which a negligibly reddened nonthermal continuum dominates in the optical (Ward *et al.* 1987, "class A"). The data are given in Table 6 and are plotted as R_L versus α_E in Figure 9.

The energy range of the SSS (0.7–3.5 keV) overlaps with that of the IPC. Six of the seven SSS points follow the α_E-R_L relation found for the IPC sample (Fig. 7). This agrees with the correlation between IPC and SSS spectral indices found by Elvis *et al.* (1986, their Fig. 5) and suggests that even hard X-ray selected objects show the R_L dependence at low energies. Energy range rather than the selection effects suggested by Elvis *et al.* (1986) seems to be the cause of the different X-ray spectra seen by the IPC and *HEAO 1* A-2.

The higher energy (2–10 keV) *HEAO 1* A-2 slopes cluster around $\alpha_E = 0.7$ and show no trend of α_E with R_L. In particular, the radio-quiet objects have $\alpha_E \sim 0.7$, flatter than similar IPC measured quasars. There are two simple explanations for the difference between the A-2 and IPC/SSS samples: either the *HEAO 1* A-2 AGNs have flatter spectra over the whole 0.1–10 keV range or all AGNs have two components, the flatter being dominant above ~ 2 keV. In the first case, the selection by *HEAO 1* A-2 of the brightest 2–10 keV sources

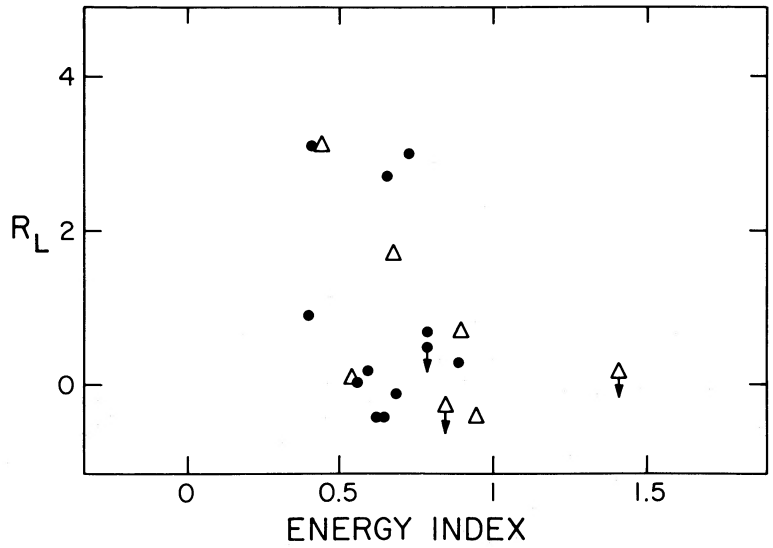

FIG. 9.—Radio loudness R_L as a function of α_E for hard X-ray selected samples of *Einstein* SSS (*triangles*) and *HEAO 1* A-2 (*filled circles*)

naturally explains the bias toward flatter slopes for this AGNs sample (Elvis *et al.* 1986). Alternatively, in a two-component model with the break point dependent upon R_L, the 2–10 keV energy band of *HEAO 1* A-2 will be dominated by the flatter component for any AGNs sample. We discuss these possibilities in the next section.

f) Two Components

Any model which tries to explain the X-ray emission of quasars must now be able to reproduce the wide range of observed soft X-ray slopes and the strong link of these slopes to the radio loudness of the quasars, as well as reproduce the narrower range of slopes found at higher energies. The apparently smooth change of X-ray spectral index α_E with radio loudness, R_L (Fig. 7), suggests, as mentioned in the previous section, the following two alternatives: (1) we are seeing two emission mechanisms, the flatter of which is linked to radio emission, mixed in different proportions along the correlation; (2) we are witnessing an intrinsic change of slope in a single mechanism. In this latter case, the pivot point must be at lower energies than the IPC band to explain the higher X-ray luminosity of the radio-loud (flatter) quasars. A third alternative is not ruled out by the IPC data: that (3) there is no smooth change in α_E, and we are instead seeing two distinct classes of quasars, radio-loud and radio-quiet quasars which have different X-ray spectra. Such a dichotomy is suggested by the two-peaked distribution in R_L found by Kellerman *et al.* (1987) for PG quasars. In either this or the "two-components" alternative, the slope of the radio-linked component must be usually ~ 0.5 and of the other, ~ 1.0. Given the errors on the IPC slope estimation these could be "universal" values, but this is certainly not required.

A reconciliation of the IPC and *HEAO* 1 A-2 results can be understood in terms of two components more easily than by the other two possibilities. Important points that must be explained are:

1. There are "flat" spectrum, radio-quiet active galaxies at high (A-2) energies.
2. The slopes of these "flat" spectrum, radio-quiet active galaxies are steeper than those of radio-loud objects at low (IPC) energies.
3. There are no "steep" spectrum, radio-loud active galaxies at high energies (only three A-2 objects are radio loud so this is not a highly significant result).

The "two-populations" model cannot explain the existence of "flat" spectrum, radio-quiet active galaxies. These objects are also the major problem for the one-component model with variable slope since this slope will be the same in all energy bands.

In contrast, the "two-component" model can explain all three of the above points. In the IPC quasars, as the relative strength of the flat component, $f_{\rm flat}$, increases, R_L increases rapidly, $R_L \propto f_{\rm flat}^{4-5}$, and the apparent X-ray slope flattens. For the radio-quiet objects ($R_L < 1$), the steep component dominates, giving $\alpha_E \sim 1$. The higher energy range of A-2 results in a significant flat component contribution at lower values of R_L and leads to flatter apparent slopes for radio-quiet active galaxies. The *HEAO 1* A-2 data are consistent with being a mixture of two components with slopes of 0.5 and 1.0. For Mrk 509, one of the best observed *HEAO 1* A-2 AGNs, a fit with two power laws of slopes 0.5 and 1.0 gives the same χ^2 as a one–power-law fit. The relative normalizations of two components at 1 keV lie within a factor 2 of each other, with the flatter component being weaker (R. F. Mushotzky, private communication).

An additional test of the two-component model is to look to energies above the A-2 range where the flat component should dominate. Rothschild *et al.* (1983) report 12–165 keV spectra for eleven AGNs observed with the *HEAO 1* A-4 experiment. Individually, a power law fitted to each galaxy spectrum gives a result entirely consistent with an extrapolation of the lower energy slopes determined by *HEAO 1* A-2. However, the errors on each measurement are ± 0.3 or worse, so that a difference between the 0.65 slope in the A-2 data and the ~ 0.5 of our two-component model is indiscernible. The only exception is NGC 4151 for which the two data sets give 1.50 ± 0.02 (A-2) and 1.53 ± 0.07 (A-4), in agreement with our model. In Figure 10 we plot the difference between the best-fit A-4 and A-2 slopes as a function of the A-2 slope. The 90% errors have been naively combined as an rms. The mean difference in Figure 10 is in the sense of a flattening of the spectrum to higher energies. A weighted mean (omitting NGC 4151) gives a difference of -0.14 ± 0.02. This implies a high energy slope ~ 0.5, in remarkable agreement with the value needed by our two-component model. To some extent this must be fortuitous, but it is clear that the *HEAO* 1 A-4 data do not rule out this simple model.

In addition, the agreement of the SSS points with the IPC α_E versus R_L relation favors a two-component model. These quasars have soft X-ray slopes steeper than their higher energy slopes, despite being hard X-ray selected.

Two components also allow quasars to contribute strongly to the diffuse X-ray background since they can both match its slope and make a substantial contribution above a few keV. This may or may not be an argument in favor of the two-component model. The normalization of the flat component is lower than the total 2 keV flux density, increasing the amount of evolution required to match the background. This topic will be discussed by Tucker and Schwartz (1987).

The infrared to X-ray continuity suggested by Elvis *et al.* (1986) would make a two-component model conceptually simpler by bringing some coherence to the overall radio to X-ray continua of quasars. A single power-law component would then explain both the infrared and soft X-ray continua of radio-quiet quasars, and a second separate component would explain the radio and hard X-ray spectra.

g) Ultrasoft Excesses and the α_E versus R_L Correlation

The $N_{\rm H}$ deficit discussed in § III*a* shows that a single component power-law fit is not an adequate description of the IPC data. Taken with the "two-component" model required by the combination of A-2 and IPC data in the previous section, a total of three X-ray emitting components seem to be needed in the kilovolt range, all of similar luminosities. Given the low spectral resolution of the IPC this may seem to be a bold claim. An alternative suggestion is that the two effects—the $N_{\rm H}$ deficit and the range of power-law slopes that correlate with R_L—are connected. Both effects might be explicable in terms of just two components: a steep ($\alpha_E \sim 3$) soft component which depends upon R_L and a flat ($\alpha_E \sim 0.5$) hard component. No $\alpha_E \sim 1.0$ component would be required in this picture.

The limited IPC resolution makes it impossible to rule out such a model through direct two-component fitting. Useful constraints can only be obtained by arbitrarily fixing the $N_{\rm H}$ or by prespecifying the two–power-law indices. Less direct tests, however, suggest that our proposed three–component model is

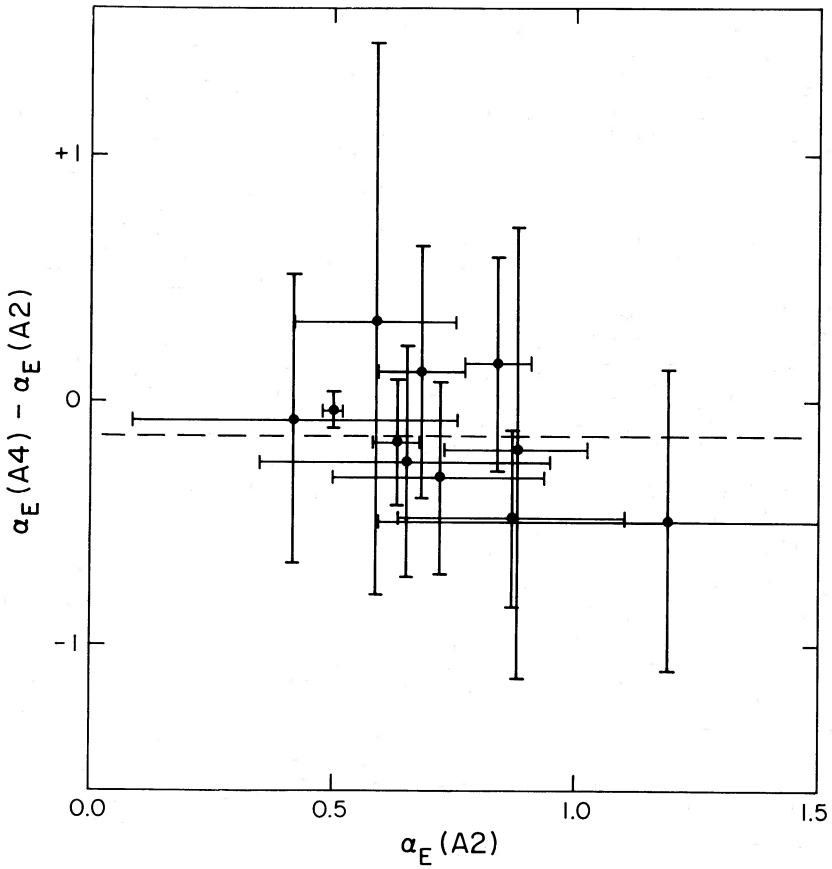

FIG. 10.—Difference between best-fit A-2 and A-4 slopes (Rothschild *et al.* 1983) plotted against A-2 slope. Numbers less than zero indicate flattening to higher (A-4) energies. Dashed line shows mean difference weighted according to signal-to-noise ratio.

more likely to be appropriate. We have fitted the X-ray spectrum over the energy range 0.6–3.5 keV for the highest signal-to-noise objects in our sample (five radio-loud and five radio-quiet). This range contains $< 15\%$ of the low-energy (<0.28 keV) photons. In a two-component model this high-energy data should be dominated by the flat, hard component for all the quasars. The results including 90% confidence limits, are summarized in Table 7. Allowing α_E, N_H to vary without restriction, six of the quasars show a steeper slope over that fitted to the full energy range. For the remaining four (three radio-loud) the slope is unchanged. However the poor constraints on N_H due to the lack of low-energy photons is likely to artificially steepen the fitted slope. We therefore also tabulate the limits on the slope while constraining N_H to be within the 90% confidence limits of the Galactic column density. In this case, the slopes remain close to the same as in the fit to all the IPC data, the slight steepening in a few cases being well within the quoted 90% confidence limits.

TABLE 7

SPECTRAL FITS FOR ENERGY RANGE 0.6–3.5 keV

Object	PHA Channels	α_E	$\alpha_E(N_H$ = Galactic)
0026+129	3–9	$0.9^{+0.9}_{-0.3}$	$0.8^{+0.2}_{-0.2}$
0205+024	4–10	$1.9^{+3.0}_{-1.0}$	$1.5^{+0.4}_{-0.3}$
0923+392	5–11	$0.3^{+2.0}_{-0.3}$	$0.4^{+0.5}_{-0.4}$
1028+313	3–9	$0.5^{+0.6}_{-0.2}$	$0.7^{+0.3}_{-0.3}$
1137+661	5–11	$2.6^{+1.0}_{-1.7}$	$0.9^{+0.2}_{-0.1}$
1219+756	5–11	$2.0^{+2.0}_{-1.0}$	$0.9^{+0.1}_{-0.1}$[a]
1226+023	4–10	$0.4^{+0.5}_{-0.2}$	$0.5^{+0.2}_{-0.2}$
1253−055	5–11	$1.3^{+0.7}_{-0.9}$	$0.6^{+0.2}_{-0.2}$
1426+015	4–9	$1.2^{+1.4}_{-0.6}$	$1.0^{+0.3}_{-0.2}$
1613+658	5–12	$2.1^{+0.8}_{-1.2}$	$1.1^{+0.3}_{-0.2}$

[a] Galactic $N_H < 90\%$ contours, nominal ± 0.1 errors adopted.

Thus our IPC data show no evidence for a single high-energy slope. The ultrasoft excess is generally at low enough energies that its presence does not affect the derived power-law fit. In addition there is no evidence for a dependence of the N_H deficit on R_L as would be expected in a two-component model (see § III*a*). We conclude that the α_E-R_L correlation is due to a change in the high-energy IPC slope. Extension of our analysis to include the higher energy MPC data for these quasars, where this is available, will provide an additional test. This analysis is underway and will be reported in a later paper.

h) Emission Mechanisms

We will briefly outline a number of possible emission mechanisms which could explain the interpretation of the α_E-R_L correlation as a mix of a steep "radio-quiet" component and a flat "radio-loud" component. We assume that a $\alpha_E \sim 1$ power law is present in all objects. (The well-known UV bump is assumed to be due to an entirely separate mechanism which we do not discuss; neither do we consider the ultrasoft excess.) Elvis *et al.* (1986) discuss possible emission mechanisms for the $\alpha_E \sim 1$ component on the assumption that it is a continuation of the

infrared power law. Here we discuss the origin of the flatter component.

Probably the most commonly discussed mechanism for linking radio and X-ray emission is synchrotron self-Compton where high-energy radio photons are Compton scattered up to X-ray energies. In its simplest form this model has a single component: a radio-quiet quasar spectrum from IR to X-ray is that of a pure synchrotron source with a high self-absorption frequency in the millimeter region and negligible Compton scattering. By reducing the magnetic field, the self-absorption frequency is reduced, yielding a radio-loud quasar with a Compton-scattered X-ray component. However, the radio spectrum would then be a continuation of the infrared power law and would not turn over in the millimeter region, as is observed (unless the electron spectrum breaks conveniently at just the right frequency). The X-ray component would also have the same steep slope as the radio emission.

The observed turnover in the millimeter region can be explained by a single inhomogeneous synchrotron source (Marscher 1977). With a suitable choice of radial density profile, overlapping spectra with different self-absorption frequencies combine to produce an apparently smooth turnover. However, in a single component model, each part of the inhomogeneous region is assumed to have the same electron energy distribution, i.e., that producing the $\alpha_E \sim 1$ infrared power law. Thus, there is no initial synchrotron spectrum which matches the flatter X-ray slope. The observed X-rays could not then be due to Compton scattering of any of the radio components.

Thus it seems that in a synchrotron self-Compton model more than one component is necessary. In this case, the radio-loud component(s) can have a flatter electron energy distribution which can then match the X-ray slope. The radio component must again be either multiple or inhomogeneous to produce the observed smooth turnover in the millimeter band as discussed above.

Synchrotron self-Compton models have the advantage of linking naturally the radio continuum and the flat X-ray component. Since the radio component changes by factors of 10^{4-5} (relative to the optical/infrared) while the flat X-ray component need change by only a factor of ~ 10, it seems plausible that the X-ray continuum is primary while the radio emission is secondary in some way. The radio luminosity is also small compared with the X-ray luminosity even in the most radio-loud quasars (e.g., 3C 273; see Elvis, Czerny, and Wilkes 1987). Pair production models (Zdziarski and Lightman 1985; Svensson 1986; Fabian *et al.* 1986) treat the hard X-ray emission as primary. However, none of these papers have considered so far whether radio emission would be a consequence of their models. Pair models have some difficulty explaining the $\alpha_E \sim 1$ slopes of radio-quiet quasars, since 0.9 appears to be the steepest slope they can produce. This would only be a problem in a one-component model for the X-ray emission where the full range of observed slopes must be explained. In a two-component model only the flat component ($\alpha_E \sim 0.5$) need be due to pair related processes.

IV. CONCLUSIONS

We have presented *Einstein* IPC soft X-ray spectra for a total of 33 quasars. These spectra show a wide variety of power-law slopes from -0.2 to 1.8. The radio loudness (R_L) is the best predictor of this X-ray slope. Radio-loud quasars ($R_L > 1$) have flatter slopes ($\alpha_E \sim 0.5$) than do radio-quiet ($R_L < 1$) quasars ($\alpha_E \sim 1.0$). The best-fit IPC slopes do not change when the lowest energy data are excluded. The *Einstein* SSS AGNs fit the α_E-R_L relation of the IPC quasars. The *HEAO 1* A-2 AGNs on the other hand show no dependence of α_E with R_L. Consideration of the IPC and *HEAO 1* A-2 results together indicates that the correlation of α_E and R_L is due to a changing mix of two components, one with $\alpha_E \sim 0.5$, the other with $\alpha_E \sim 1.0$. The break point between the two components falls within the 2–10 keV *HEAO* 1 A-2 band for radio-quiet quasars.

There is a clear tendency for the X-ray measured column densities to be lower than the Galactic line-of-sight values. This deficit is unlikely to be due to sample selection. A comparison with BL Lac objects shows that the effect is intrinsic to the quasars. The only obvious explanation is an upturn in the X-ray spectra in the $\lesssim 0.28$ keV region forming an " ultra-soft excess " in addition to the two components discussed above. Interpretation of this excess as the high-energy tail of the blue bump in quasars provides a consistent picture, since BL Lac objects have no blue bump.

Thus the simplest model that incorporates both the IPC and *HEAO 1* A-2 results comprises three X-ray components: a flat ($\alpha_E \sim 0.5$) power law that dominates in all quasars above a few keV and radio-loud quasars above ~ 0.5 keV; a steeper ($\alpha_E \sim 1.0$) power law that dominates in the 0.5–3.5 keV IPC range in the radio-quiet majority of quasars; and a very steep ($\alpha_E \sim 2$–3) component that becomes important only below ~ 0.3 keV in all but a handful of objects. This scheme has some advantages: all quasars would have the same flat component, removing the need to explain why radio-loud quasars favor slopes of 0.5 (IPC) and radio-quiet quasars, slopes of 0.7 (A-2); this flat component would allow quasars to match the diffuse X-ray background spectrum; the $\alpha_E \sim 1.0$ component is consistent with an extension of the infrared power law; the very steep component could have several different causes but its interpretation in terms of emission from the hot innermost region of an accretion disk is appealing.

The IPC sample does not include the full range of quasar X-ray properties. It is biased against quasars with high total absorbing column and those with steep slopes, but it is unclear at what α_E and N_H these effects become important. Simulations are underway to help define the limits of our study. The absence of X-ray spectra for quasars with $\alpha_{ox} > 1.5$ is a serious lack. Are these X-ray sources weak because they are heavily absorbed, because they have very steep X-ray spectra, or because they have "normal" X-ray spectra with low normalization? We need X-ray spectra of complete well-defined samples of quasars. Only then can we answer these questions and, in addition, make definite statements on emission-line cloud-covering factors and on the normal interstellar absorption of the presumed host galaxies. Complete samples extending to large α_{ox} objects will also allow a better test of the single infrared to X-ray power-law hypothesis.

Altogether, the soft X-ray spectra of quasars have shown a surprising richness and some intriguing regularities. They will have significant effects on theories of quasar continuum emission and offer an interesting alternative interpretation to previously known differences between radio-quiet and radio-loud quasars. This sample will now form the basis for our study of the complete quasar energy distributions.

We wish to thank G. Fabbiano, G. Madejski, R. Mushotzky, M. Urry, G. Zamorani, and A. Zdziarski for useful discussions. We are grateful to K. Kellerman for permission to use his radio data in advance of publication. We thank S. Gibbs and especially C. Poux for assistance in data analysis. This work was supported in part by NASA contract NAS8-30751.

REFERENCES

Agrawal, P. C., Riegler, C. R., and Mushotzky, R. F. 1979, *Ap. J. (Letters)*, **233**, L47.
Arnaud, K. A., *et al.* 1985, *M.N.R.A.S.*, **217**, 105.
Angel, J. R. P., and Stockman, H. S. 1980, *Ann. Rev. Astr. Ap.*, **18**, 321.
Avni, Y., and Tananbaum, H. 1986, *Ap. J.*, **305**, 83.
Bechtold, J., Czerny, B., Elvis, M., Fabbiano, G., and Green, R. F. 1986, *Ap. J.*, **314**, 699.
Berrington, K. A., Burke, P. G., Fon, W. C., and Taylor, K. T. 1982, *J. Phys. B*, **15**, L603.
Bezler, M., Kendziora, E., Staubert, R., Hasinger, G., Pietsch, W., Reppin, C., Trümper, J., and Voges, W. 1984, *Astr. Ap.*, **136**, 351.
Bowyer, S. 1986, *Adv. Space Res.*, **6**, 153.
Branduardi-Raymont, G., Mason, K. O., Murdin, P. G., and Martin, C. 1986, *M.N.R.A.S.*, in press.
Branduardi-Raymont, G., *et al.* 1987, in preparation.
Brown, R. L., and Gould, R. J. 1970, *Phys. Rev. D*, **2**, 2252.
Canizares, C. R., and Kruper, J. 1984, *Ap. J. (Letters)*, **278**, L99.
Carleton, N. P., Elvis, M., Fabbiano, G., Willner, S. R., Lawrence, A., and Ward, M. J. 1987, *Ap. J.*, in press.
Elsmore, B., and Ryle, M. 1976, *M.N.R.A.S.*, **174**, 411.
Elvis, M., Czerny, B., and Wilkes, B. J. 1987, in *The Physics of Accretion onto Compact Objects*, ed. K. O. Mason, M. G. Watson, and N. E. White (Berlin: Springer-Verlag), p. 389.
Elvis, M., Green, R. F., Bechtold, J., Schmidt, M., Neugebauer, G., Soifer, B. T., Matthews, K., and Fabbiano, G. 1987, *Ap. J.*, **310**, 291.
Elvis, M., Wilkes, B. J., and Tananbaum, H. 1985, *Ap. J.*, **292**, 357.
Fabian, A. C., Blandford, R. D., Guilbert, P. W., Phinney, E. S., and Cuellar, L. 1986, *M.N.R.A.S.*, **221**, 931.
Feigelson, E. D., Isobe, T., and Kembhavi, A. 1984, *A.J.*, **89**, 1464.
Giacconi, R., *et al.* 1979, *Ap. J.*, **230**, 540.
Gioia, I. 1986, private communication.
Gorenstein, P., Harnden, R. F., and Fabricant, D. 1981, *IEEE Trans. Nucl. Sci.*, **NS-28**, 869.
Gower, A. C., and Hutchings, J. B. 1984, *A.J.*, **89**, 1658.
Hargrave, P. J., and McEllin, M. 1975, *M.N.R.A.S.*, **173**, 37.
Harnden, R. F., Fabricant, D. G., Harris, D. E., and Schwarz, J. 1984, *Smithsonian Ap. Obs. Spec. Rept.*, No. 393, p. 8.
Hewitt, A., and Burbidge, G. 1987, *Ap. J. Suppl.*, **63**, 1.
Hoag, A. A., Thomas, N. G., and Vaucher, B. G. 1982, *Ap. J.*, **263**, 23.
Hutchings, J. B., and Gower, A. C. 1985, *A.J.*, **90**, 405.
Johnson, H. L. 1986, *Ann. Rev. Astr. Ap.*, **4**, 193.
Kellermann, K. I., Sramek, R., Shaffer, D., Green, R., and Schmidt, M. 1986, *IAU Symposium 119, Quasars*, ed. G. Swarup and V. K. Kapahi (Dordrecht: Reidel), p. 95.
Kellermann, K. I., Sramek, R., Shaffer, D., Green, R., and Schmidt, M. 1987, in preparation.
Kembhavi, A. 1985, *IAU Symposium 119, Quasars*, ed. G. Swarup and V. K. Kapahi (Dordrecht: Reidel), p. 239.
Lockman, F. J., Hobbs, L. M., and Shull, J. M. 1986, *Ap. J.*, **301**, 380.
Madejski, G. M. 1985, Ph.D. thesis, Harvard University.
Maraschi, L., Roasio, R., and Treves, A. 1982, *Ap. J.*, **253**, 312.
Marscher, A. P. 1977, *Ap. J.*, **216**, 244.
McAlary, C. W., McLaren, R. A., McGonegal, R. J., and Maza, J. 1983, *Ap. J. Suppl.*, **52**, 341.
Morrison, R., and McCammon, D. 1983, *Ap. J.*, **270**, 119.
Mushotzky, R. F. 1984, *Adv. Space Res.*, **3**, 157.
Neff, S. C., and Browne, R. L. 1984, *A.J.*, **89**, 195.
Osterbrock, D. E. 1977, *Ap. J.*, **215**, 733.
Owen, F. N., Helfand, D. J., and Spangler, S. R. 1981, *Ap. J. (Letters)*, **250**, L55.
Pagel, B. E. J. 1982, *Phil. Trans. Roy. Soc. London, A*, **307**, 19.
Pauliny-Toth, I. T. K., Kellermann, K. I., Davies, M. M., Fomalont, E. B., and Shaffer, D. B. 1972, *A.J.*, **77**, 265.
Perley, R. A. 1982, *A.J.*, **87**, 859.
Peterson, B. M., Foltz, C. B., and Byard, P. L. 1981, *Ap. J.*, **251**, 4.
Petre, R., Mushotzky, R. F., Krolik, J. H., and Holt, S. S. 1984, *Ap. J.*, **280**, 499.
Pooley, G. G., and Henbest, S. N. 1974, *M.N.R.A.S.*, **169**, 477.
Pounds, K. A., Stanger, V. J., Turner, T. J., King, A. R., and Czerny, B. 1986, *M.N.R.A.S.*, **224**, 443.
Raymond, J., and Smith, B. W. 1977, *Ap. J. Suppl.*, **35**, 419.
Rothschild, R. E., Mushotzky, R. F., Baity, W. A., Gruber, D. E., Matteson, J. L., and Peterson, L. E. 1983, *Ap. J.*, **269**, 423.
Rudnick, L., Sitko, M. L., and Stein, W. A. 1984, *A.J.*, **89**, 753.
Savage, A. 1976, *M.N.R.A.S.*, **174**, 259.
Schmidt, M., and Green, R. F. 1983, *Ap. J.*, **269**, 352.
———. 1986, *Ap. J.*, **305**, 68.
Shimmins, A. J., and Bolton, J. G. 1972, *Australian J. Phys. Ap. Suppl.*, No. 23, p. 1.
Sramek, R. A., and Tovmassian, H. M. 1975, *Ap. J.*, **196**, 339.
Stark, A. A., Heiles, C., Bally, J., and Linke, R. 1987, in preparation.
Svensson, R. 1986, in *IAU Colloquium 89, Radiative Hydrodynamics in Stars and Compact Objects*, ed. D. Mihalas and K.-H. Winkler (*Lecture Notes in Physics*, **255**).
Tananbaum, H., Wardle, J. F. C., Zamorani, G., and Avni, Y. 1983, *Ap. J.*, **268**, 60.
Tananbaum, H., Avni, Y., Green, R. F., Schmidt, M., and Zamorani, G. 1986, *Ap. J.*, **305**, 57.
Tucker, W., and Schwartz, D. A. 1987, in preparation.
Ulvestad, J. S., and Wilson, A. S. 1984, *Ap. J.*, **278**, 544.
Unger, S., Lawrence, A., Wilson, A. S., Elvis, M., and Wright, A. E. 1987, *M.N.R.A.S.*, in press.
Urry, C. M., Mushotzky, R. F., and Holt, S. S. 1986, *Ap. J.*, **305**, 369.
Véron-Cetty, M.-P., and Véron, P. 1984, *ESO Sci. Rept*, No. 1, p. 1.
Wall, J. V. 1972, *Australian J. Phys. Ap. Suppl.*, No. 32, p. 1.
Ward, M. J., Elvis, M., Fabbiano, G., Carleton, N. P., Willner, S. P., and Lawrence, A. 1987, *Ap. J.*, in press.
Wilkes, B. J., Elvis, M., and McHardy, I. 1987, *Ap. J. (Letters)*, in press.
Worrall, D. M., and Marshall, F. E. 1984, *Ap. J.*, **276**, 434.
Worrall, D. M., Giommi, P., Tananbaum, H., and Zamorani, G. 1987, *Ap. J.*, **313**, 596.
Zamorani, G., *et al.* 1981, *Ap. J.*, **245**, 357.
Zdziarski, A. 1986, *Ap. J.*, **303**, 94.
Zdziarski, A., and Lightman, A. P. 1985, *Ap. J. (Letters)*, **294**, L79.

M. ELVIS and B. J. WILKES: Harvard-Smithsonian Center for Astrophysics, 60 Garden Street, Cambridge, MA 02138